

## Reply to Anonymous Referee

Thanks for the reviewer's helpful comments. We have given our point-to-point response to your comments in the revised manuscript.

In order to carefully address the comments, we made extensive model experiments, including (1) We have simulated the case during the 2017-2018 winter (January 2018 as a baseline simulation), and also added a sensitivity experiment that air temperature is 2°C higher than that in January 2018.

(2) As required by the reviewer (although this is not the focus of the study), we also studied the impact of a decrease of 2°C over the Tibetan Plateau on the air quality in the Sichuan Basin, via designing a set of experiments that air temperature respectively decreases by 2°C during the 2013-2014 and 2017-2018 winters.

(3) To address the reviewer's comment, we have added two new experiments that air temperature increases by 0.5°C, 1.0°C during the 2013-2014 winter, to give a general evaluation for the contribution of the warming plateau on the air quality in the basin.

The detailed explanation of these new model runs is given in the revised paper and in this response. We believe that these extensive new model runs will significantly enhance the quality of the paper.

### General comments:

Thanks to the authors for their efforts on this manuscript. The results sound reasonable. The increment of 2C degree have resulted in a weaker winter Tibetan Plateau Monsoon, which may induce decreased high-pressure system at the surface over the TP and decreased air flows from the TP to the Sichuan Basin. The decreased air flows, therefore, was the dominant reason for the improvement of air quality in the Sichuan Basin. However, I will not recommend publication for this manuscript at current condition.

### Major comments:

**Comment 1.** I wonder whether the simulations are greatly dependent on simulation background. The authors compared the baseline simulation and sensitivity simulations during DJF from 2013-2014. How about the similar simulations during winter in other years? I suggested that the authors may compare a sensitive experiment with baseline experiment by using initial and boundary data in winter from 2017-2018. In these experiments, a decrease of

2C degree can be set in the sensitivity experiment. If the simulations could provide a worse air quality in the Sichuan Basin, that will be fine.

**Response:** Your comment is right, and the simulation is dependent of the simulation background, but not greatly. We have simulated the case during the 2017-2018 winter (January 2018 as a baseline simulation), and also added a sensitivity experiment that air temperature is 2°C higher than that in January 2018. The results are somewhat different from those in January 2014, but the conclusions are consistent. We added Figures S7-S8, Figure S10, Figure S12 in supplementary materials to make sure of a robust conclusion.

In order to respond to the reviewer's comment about the impact of a decrease of 2°C over the TP on the air quality in the Sichuan Basin during the 2017-2018 winter, we also design a set of experiments that air temperature respectively decreases by 2°C during the 2013-2014 and 2017-2018 winters. However, impacts of a warming TP (air temperature increases by 2°C) and a cooling TP (air temperature decreases by 2°C) on the air quality in the Sichuan Basin are actually two studies, and these two impacts are not necessarily opposite completely. There are too many influence factors relate to air quality, and the air temperature and its influence on other factors are only some of them. In fact, the key factors such as winds, RH and PBLH discussed in our study plays important roles in modulating air quality.

Here we investigate the impact of a warming plateau, and the impact of a cooling plateau is out of the scope in our study. To address the reviewer's comment, results of the impact of a cooling plateau on air quality in the basin are followed (Figures 1-4), but not shown in the revised manuscript.

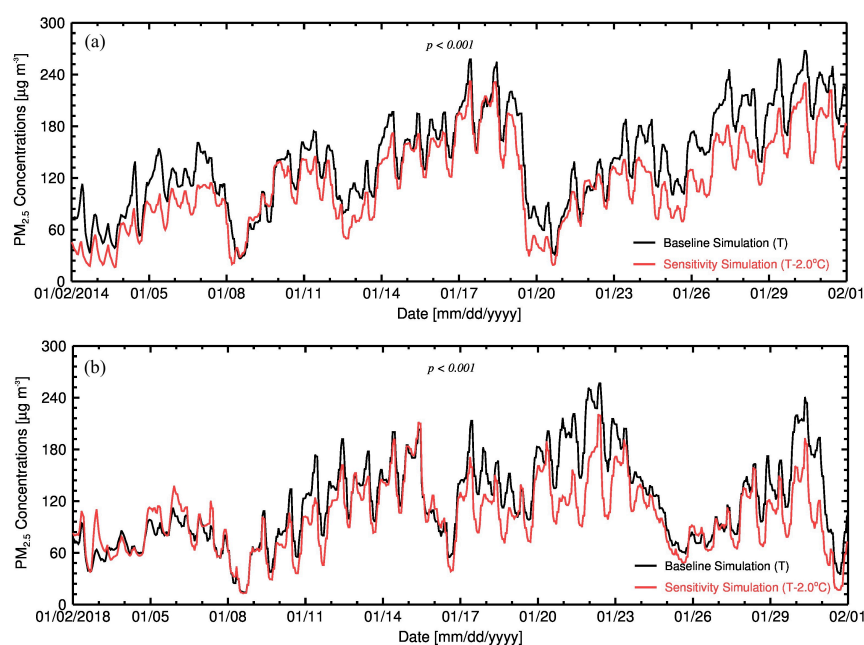


**Figure 1** Time series of PM<sub>2.5</sub> concentration over the basin, the baseline simulation is selected in January

2014 and January 2018, in which the 2°C cooling occur over the plateau relative to the baseline simulation. The differences in PM<sub>2.5</sub> concentrations between the baseline simulation and sensitivity simulations are significant, exceeding 99.9% confidence level ( $p < 0.001$ ).

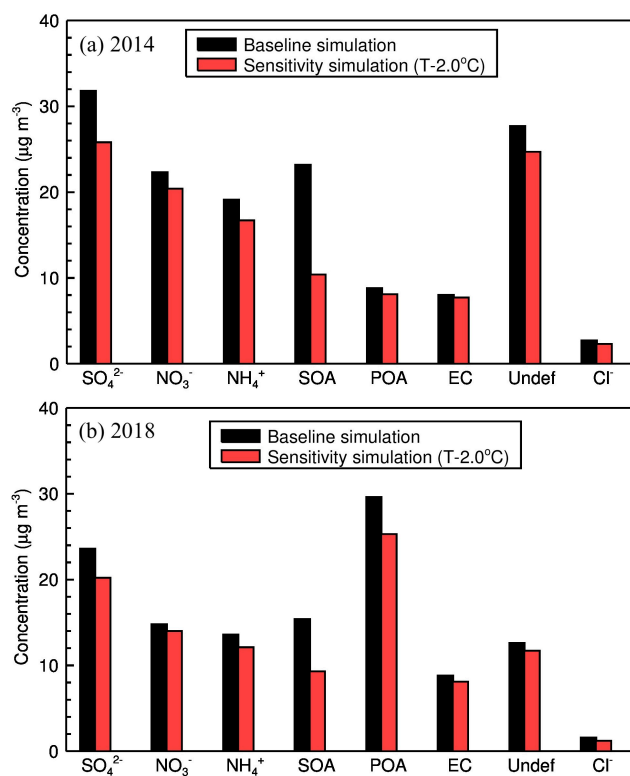


**Figure 2** Comparisons of PM<sub>2.5</sub> chemical composition in the basin with (sensitivity simulation, red bar) and without (the baseline simulation, black bar) the 2.0°C cooling.

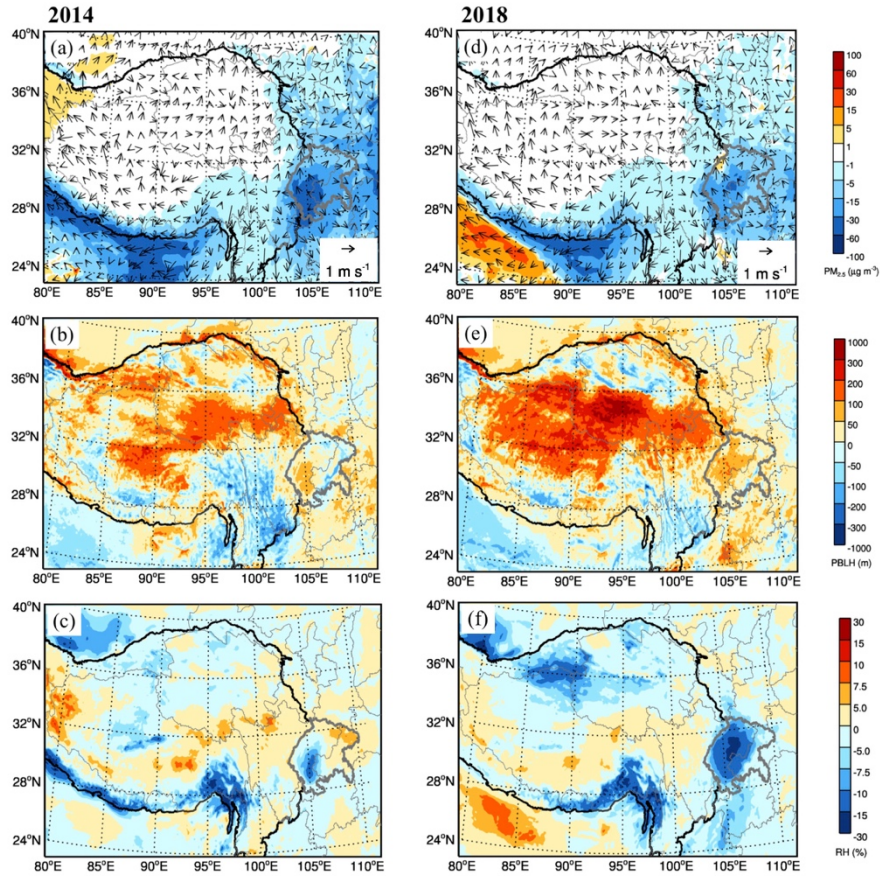


**Figure 3** Differences in spatial distributions of surface  $PM_{2.5}$  concentration and meteorological parameters (winds, PBLH and RH) between the baseline simulation and sensitivity simulation when the plateau cools by  $2.0^{\circ}C$ . (a) - (c) for the 2013-2014 winter. (d) - (f) for the 2017-2018 winter.

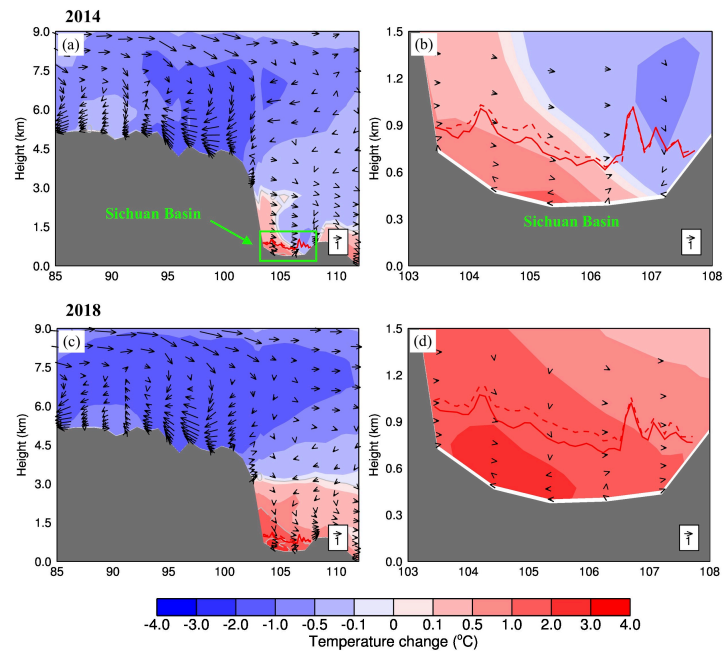


**Figure 4** Vertical profiles of changes in temperature (shading and gray contour) and winds (arrows) along  $30^{\circ}N$  when the plateau cools by  $2^{\circ}C$ . The gray shaded area presents topography. The green box for the

Sichuan Basin, and the red solid (baseline simulation) and dash (sensitivity simulation) lines for the PBL height. (a) - (b) for the 2013-2014 winter, and (c) - (d) for the 2017-2018 winter.

Figure 1 shows that a cooling plateau also leads to a reduction of PM<sub>2.5</sub> concentration in the basin, and both the primary and secondary aerosols in PM<sub>2.5</sub> decrease when the plateau cools by 2°C (Figure 2). Here referring to the impact of a warming plateau, we briefly analyze the reason why PM<sub>2.5</sub> concentration decreases in the basin (Figures 3-4). In comparison with results from a warming and a cooling plateau, the significant differences are from the pressure change. Definitely, changes in the wind fields induced by the pressure change are opposite over the eastern plateau and the basin under these opposite circumstances (Figure 3a and Figure 3d, Figure 4). Nonetheless, wind changes both have enhanced the transport of pollutants in the Sichuan Basin to the surrounding regions, regardless of whether the plateau is warming or cooling.

The significant impact of the cooling or warming over the Tibetan Plateau on the basin concentrates on the temperature change. We found that a warming plateau is conducive to a cooling basin (Figure 10, Figures S11-12 in our study), vice versa, a cooling plateau is conducive a warming basin (as shown here). We speculate that the change of pressure gradient induced by the temperature change can explain the cause-to-effect relationship, referring to the text in Lines 349-354: *“We speculate that changes in the surface pressure can account for the maximal temperature reduction here. After the warming, surface pressure decreases in the basin (Figure 8, Figure S9b and Figure S9f, Figure S10b), which produces more convergent airflow (as shown in Figure 7, Figure S9a and Figure S9e, Figure S10a). The strengthened convergent airflow induces an intensified ascending motion, conducive to a reduction of temperature in the basin.”*

Changes in the RH and PBLH within the basin due to the temperature change over the plateau are not significant, so differences in the impacts of the changed RH and PBLH in the basin on air quality are not significant. In summary, air quality is all improved when the plateau is warming or cooling, this is mainly because that changes in winds are conducive to pollutants' transport. Changes in the RH and PBLH are conducive to PM<sub>2.5</sub> reduction in the basin.

**Comment 2.** In the model, the authors set to the 2°C warming at all grids covering the TP in the initial and boundary fields. However, this condition has not been considered for regions surrounding the TP. Have you considered gradual decrease in air temperature from the TP to the surrounding regions of the TP in the model?

**Response:** Yes, we considered that the temperature change follows the change in the true case, however, it is hardly to achieved it.

First of all, the settings of vertical layers and intervals are different between the model and reanalysis data, and we cannot accurately match them consistent with the true vertical profile of air temperature change. Secondly, we aim to calculate the impact of a warming plateau on air quality in the basin, so the warming in the surrounding regions of the plateau is not allowed to be considered. If we also consider the warming in these regions, we cannot separate the impact of the plateau and surrounding regions. Most importantly, the warming in surrounding regions is not significant (Figure 3 in the revised version), so the temperature from the plateau to the basin is not gradually decreased.

Thus, we select an average temperature change over the plateau as a sensitivity experiment to explain a warming plateau on the air quality in the basin.

**Comment 3.** Would you like to give general evaluation for the contribution of the warming of the TP on the air quality in the Sichuan Basin? For instance, when the air temperature increases by 0.5 degree or 1 degree, I wonder whether the air quality in the Sichuan Basin will be improved.

**Response:** We have added three new experiments that air temperature increases by 0.5°C, 1.0°C during the 2013-2014 winter, and air temperature increases by 2.0°C during the 2017-2018 winter over the plateau. Results show that air quality in the basin is also improved, consistent with the conclusion summarized in the original text. We added the results in Figs 5-6, Figures S6-S12 in Supplementary materials in the revised version.

The re-written text is also added in the revised manuscript:

**Key points**, Lines 21-25: *A warming plateau leads to an enhanced easterly wind, an increased PBLH and a decreased RH in the Sichuan Basin.*

*The 2 ° C warming significantly reduces PM<sub>2.5</sub> concentration in the basin by 25.1 μg m<sup>-3</sup>, of which secondary aerosol is 19.7 μg m<sup>-3</sup>.*

**Abstract**, Lines 34-39: *Here we use the WRF-CHEM model to lay emphasis on the impact of the 2 ° C warming on air quality in the basin. The model results show that the 2 ° C warming causes an enhanced easterly wind, an increase in the Planetary Boundary Layer height (PBLH) and a decrease in the relative humidity (RH) in the basin. Enhanced easterly wind increases PM<sub>2.5</sub> transport from the basin to the plateau. The elevated PBLH strengthens vertical diffusion*

of  $PM_{2.5}$ , while the decreased RH significantly reduces secondary aerosol formation.

**Introduction**, Lines 90-103: *In Section 4, we design three sets of numerical simulations to calculate the impact of climate change on air quality. One group includes two baseline simulations in two periods (January 2014 and January 2018), which are constrained by observed surface meteorological parameters and pollutant concentrations. The second group includes three sensitivity simulations during the 2013-2014 winter, which uses the same emission inventory and meteorological fields as the baseline simulation except for the changed air temperature. We also set the third sensitivity simulation, in which the plateau is also warming, but on the basis of the period for the 2017-2018 winter.*

**Data and Methods**, Lines 166-185: *According to the meteorological records at weather stations, surface air temperature risen by an average of  $2^{\circ}C$  from 2013 to 2017 over the plateau (Table S1). ERA-interim reanalysis data also show that the troposphere (600hPa - 250hPa) over the plateau is warming during the 2013-2017 period, and the temperature increment shows a parabolic pattern with the altitude, by an average increase of  $\sim 2^{\circ}C$  (Figure S1). Thus, we design several sensitivity simulations, with an average temperature increase in the troposphere over the plateau, to assess impacts of a warming plateau on air quality in the basin. To eliminate the influence of simulation background, we conduct two baseline simulations for the 2013-2014 winter (January 2014) and the 2017-2018 winter (January 2018) as the control groups. The other two sets focus on sensitivity simulations that reflect an observational increase in air temperature over the plateau. At the year of 2014, the sensitivity simulation uses the same emission inventory and meteorological conditions as the baseline simulation except that the temperature in the troposphere over the plateau respectively increases by  $0.5^{\circ}C$ ,  $1.0^{\circ}C$  and  $2.0^{\circ}C$ . The third group is a sensitivity simulation with an increase of  $2.0^{\circ}C$  on the basis of air temperature in January 2018. In the domain, we set to the warming at all grids covering the plateau (the region surrounded by the dark line in Figure 1b) in the initial and boundary fields. In order to ensure a persistent influence of the warming, we drive the initial field with a  $0.5^{\circ}C$ ,  $1.0^{\circ}C$ , and  $2^{\circ}C$  increment every day in January 2014, and a  $2^{\circ}C$  increment every day in January 2018. Then, by comparing the difference between the sensitivity simulations and the baseline simulation, we determine the impact of the warming over the plateau on air quality in the basin.*

**Results and Discussion**, Lines 257-267: *To examine impacts of a warming plateau on  $PM_{2.5}$  concentration in winter in the basin, we set three levels of temperature increase of  $0.5^{\circ}C$ ,  $1.0^{\circ}C$  and  $2.0^{\circ}C$  over the plateau. Time series of  $PM_{2.5}$  concentrations in these simulations (with and without the warming over the plateau) are respectively calculated. The results show that  $PM_{2.5}$  concentration in the basin is significantly reduced (Figure 5). In comparison with three levels*

of temperature increase, the maximal reduction occurs in the case of 2°C warming, with an average of  $25.1 \mu\text{g m}^{-3}$  ( $p < 0.001$ ). Under the circumstance of the 2°C warming, the maximal hourly reduction reaches to  $84.6 \mu\text{g m}^{-3}$  (Figure S6a) and the maximal percentage reduction is about 64.4% (Figure S6b). We also calculate the changes in  $\text{PM}_{2.5}$  concentration and its percentage under the influence of the 2°C warming on the basis of January 2018 (Figure S7), of which the result is consistent with Figure S6, though there must inevitably be some differences in the magnitude.

Lines 275-289: To better understand the impact of a warming plateau on  $\text{PM}_{2.5}$  concentration, we also calculate changes in  $\text{PM}_{2.5}$  chemical composition in the basin. Both primary and secondary aerosols in  $\text{PM}_{2.5}$  decreases more significantly with an increase in temperature increment (Figure 6), except for the nitrate due to its competition for ammonia with sulfate (Feng et al., 2018). As a result, the more sulfate is reduced under the case of the 2°C warming, the less nitrate is reduced. As shown in Figure 6, the warmer the plateau is, the more  $\text{PM}_{2.5}$  concentration and its chemical composition in the basin decrease, suggesting that a warming plateau has increasing implications for air quality in the basin. Here we show that the maximal impact of the plateau under the case of the 2°C warming, in which secondary aerosol reduces by  $19.7 \mu\text{g m}^{-3}$ , accounting for 78.5% of the total reduction, greatly larger than the reduction of primary aerosol. For example, the largest reduction is SOA, reducing from  $23.2 \mu\text{g m}^{-3}$  in the base case to  $10.8 \mu\text{g m}^{-3}$  in the 2°C warming case. The second reduction is sulfate (from  $31.8 \mu\text{g m}^{-3}$  to  $28.6 \mu\text{g m}^{-3}$ ). The next are nitrate and ammonium ( $22.3 \mu\text{g m}^{-3}$  and  $19.1 \mu\text{g m}^{-3}$  in the base case, and  $20.2 \mu\text{g m}^{-3}$  and  $17.5 \mu\text{g m}^{-3}$  in the 2°C warming case). Significance testing of the difference in every chemical composition between the baseline simulation and the 2°C warming case is also given in Table S2.

Lines 292-295: Thus, we emphasize the impact of the 2°C warming over the plateau on  $\text{PM}_{2.5}$  concentration in the basin in our study. Meanwhile, we analyze the case for the 2017-2018 winter, in which a similar change in  $\text{PM}_{2.5}$  chemical composition is obtained when the plateau becomes 2°C warmer (Figure S8).

Lines 302 -307: Enhanced easterly winds and weakened westerly winds are both in favor of the east-to-west transport of pollutants from the basin to the plateau. We also show changes in  $\text{PM}_{2.5}$  concentration and winds under the cases of 0.5°C and 1.0°C warming in January 2014, consistent with the result of the 2°C warming, except that the reduction of  $\text{PM}_{2.5}$  concentration and the change in wind speed are fewer (Figure S9a and Figure S9e). The case in January 2018 (Figure S10a) is also similar to the result of the 2°C warming.

Lines 332-335: Our results suggest that the warming plateau plays different roles in the PBL development over the plateau and the basin. Due to the warming, the PBLH decreases in most

areas of the plateau, but it increases over the basin (Figure 9, Figure S9c and Figure S9g, Figure S10c). The maximal rise occurs under the case of the 2°C warming, by 50 - 200 m over the basin (Figure 9 and Figure S10c).

Lines 337-352: Thus, we explore the underlying cause that leads to the difference in the PBLH in the domain. The PBLH is strongly related to the changes in vertical temperature and wind, Figure 10 and Figures S11-12 display vertical profiles of changes in temperature and winds in the plateau and the basin. Results show that the warming causes a maximal warm layer around 1 km above the ground of the plateau. Noticeably, the warm layer acts as a dome covering 4.5 km above the Sichuan Basin (Figure 10a, Figure S11a and Figure S11c, Figure S12a). Xu et al. (2017) also finds out a significant warm plume extending from the plateau to the downstream Sichuan Basin and Yangtze River Delta by use of NCEP/NCAR reanalysis data. We suggest that this is probably due to a sharp topography decrease (from ~ 5 km in the plateau to < 1 km in the basin) which leads to a warm plume via subsidence. In the basin, there is a decrease in the temperature from the lower troposphere to ~ 4 km, with a maximal temperature reduction (0.5 - 2°C) located at 1.5 km to 3 km above the ground (Figure 10a, Figure S11a and Figure S11c, Figure S12a). We speculate that changes in the surface pressure can account for the maximal temperature reduction here. After the warming, surface pressure decreases in the basin (Figure 8, Figure S9b and Figure S9f, Figure S10b), which produces more convergent airflow (as shown in Figure 7, Figure S9a and Figure S9e, Figure S10a).

Lines 375-380: We examine the influence of in the RH change induced by a warming plateau on PM<sub>2.5</sub> concentration in the basin. Results show that there is remarkable change in RH in the basin due to the warming of the plateau (Figure 11, Figure S9d and Figure S9h, Figure S10d). In the baseline simulation, the RH varies in the range of 40% - 80% over the basin (Figure 11a). However, the RH varies from 50% to 70% in the 2 °C warming simulation (Figure 11b), suggesting that the basin becomes drier when the plateau is warmer.

**Conclusions**, Lines 407-411: The most significant impact of the plateau on PM<sub>2.5</sub> concentration in the basin occurs under the case of the 2°C warming. Through an enhanced horizontal transport, a reduced RH and an increased PBLH, the warming plateau significantly reduces PM<sub>2.5</sub> concentration in the basin. A larger pressure gradient from the basin to the plateau is favorable for an east-to-west transport for pollutants within the basin.

Lines 421-422. On average, PM<sub>2.5</sub> concentration reduces by 25.1  $\mu\text{g m}^{-3}$  on the basis of the 2013-2014 winter; of which the primary and secondary aerosols decrease by 5.4  $\mu\text{g m}^{-3}$  and 19.7  $\mu\text{g m}^{-3}$ , respectively.



16

17 **Key points**

18

19 The Tibetan Plateau is rapidly warming, and the temperature has risen by 2 ° C from  
20 2013 to 2017.

21

22 A warming plateau leads to an enhanced easterly wind, an increased PBLH and a  
23 decreased RH in the Sichuan Basin.

24

25 The 2 ° C warming significantly reduces PM<sub>2.5</sub> concentration in the basin by 25.1 µg  
26 m<sup>-3</sup>, of which secondary aerosol is 19.7 µg m<sup>-3</sup>.

27

28 **Abstract**

29

30 Impacts of global climate change on the occurrence and development of air pollution  
31 have attracted more attentions. This study investigates impacts of the warming Tibetan  
32 Plateau on air quality in the Sichuan Basin. Meteorological observations and ERA-  
33 interim reanalysis data reveal that the plateau has been rapidly warming during the last  
34 40 years (1979-2017), particularly in winter when the warming rate is approximately  
35 twice as much as the annual warming rate. Since 2013, the winter temperature over the  
36 plateau has even risen by 2 ° C. Here we use the WRF-CHEM model to lay emphasis  
37 on the impact of the 2 ° C warming on air quality in the basin. The model results show  
38 that the 2 ° C warming causes an enhanced easterly wind, an increase in the Planetary  
39 Boundary Layer height (PBLH) and a decrease in the relative humidity (RH) in the  
40 basin. Enhanced easterly wind increases PM<sub>2.5</sub> transport from the basin to the plateau.  
41 The elevated PBLH strengthens vertical diffusion of PM<sub>2.5</sub>, while the decreased RH  
42 significantly reduces secondary aerosol formation. Overall, PM<sub>2.5</sub> concentration is  
43 reduced by 17.5% (~25.1 μg m<sup>-3</sup>), of which the reduction in primary and secondary  
44 aerosols is 5.4 μg m<sup>-3</sup> and 19.7 μg m<sup>-3</sup>, respectively. These results reveal that the recent  
45 warming plateau has improved air quality in the basin, to some certain extent,  
46 mitigating the air pollution therein. Nevertheless, climate system is particularly  
47 complicated, and more studies are needed to demonstrate the impact of climate change  
48 on air quality in the downstream regions as the plateau is likely to continue warming.

49

50 **Keywords:** climate change, air quality, Tibetan Plateau, WRF-CHEM model

51

## 52 **1 Introduction**

53

54 The Tibetan Plateau is known as the third pole because of its high altitude and large  
55 area. It is also regarded as an important response region to the Northern Hemisphere,  
56 and even global climate due to its sensitivity to climate change. Previous studies on the  
57 Tibetan Plateau show that the region was experiencing warming in the second half of  
58 the 20<sup>th</sup> century, especially in the winter months (Kuang and Jiao, 2016; Liu and Chen,  
59 2000; Rangwala et al., 2009). The warming plateau not only plays a significant role in  
60 driving the weather and climate change, as well as the ecological system, but also has  
61 an important impact on air quality in the downstream regions. Xu et al. (2016) suggest  
62 that the thermal anomaly over the Tibetan Plateau obviously increases haze frequency  
63 and surface aerosol concentration in central-eastern China.

64

65 However, the impacts of climate change on air quality in China are still unclear. Some  
66 researches hold the opinion that climate change induced by greenhouse gas emission  
67 increases severe haze occurrence and intensity in winter at Beijing, and its impact will  
68 continue in the future (Cai et al., 2017; Zou et al., 2017). Similarly, Xu et al. (2017)  
69 suggest that climate warming anomaly in the lower and middle troposphere over the  
70 continent around the Yangtze River Delta leads to more haze days in winter during  
71 recent decades. On the contrary, another opinion suggests that climate change in the  
72 past two decades is favorable for air pollution dispersion in northern China via  
73 enhancing mid-latitude cold surges in winter (Zhao et al., 2018). If cold surge is strong  
74 enough, pollutants would be transported to the downstream regions, causing a better air  
75 quality in the upstream region but a worse one in the downstream region. Thus, there  
76 may be regional differences in the impact of climate change on air quality.

77

78 Previous studies on air pollution in China are concentrated in the developed regions,

79 such as the North China Plain, the Yangtze River Delta and the Pearl River Delta. Few  
80 studies have paid attention to the Sichuan Basin, although the region is undergoing  
81 severe air pollution, and mean PM<sub>2.5</sub> concentration is more than 110 µg m<sup>-3</sup> in winter  
82 (Qiao et al., 2019; Tao et al., 2017; Wang et al., 2018; Yang et al., 2011). Thus, it is  
83 necessary to explore the underlying causes that leads to air pollution in the Sichuan  
84 Basin.

85

86 The Sichuan Basin locates in the downstream region of the Tibetan Plateau, and its  
87 weather conditions are obviously affected by the plateau (Duan et al., 2012; Hua, 2017;  
88 Zhao et al., 2019). For instance, the foggy weather, southwest vortex and low-level  
89 shear line over the basin are closely associated with the plateau (Zhu et al., 2000). These  
90 changes in weather conditions induced by the plateau undoubtedly affect the  
91 development and dispersion of air pollution in the basin, because the huge terrain can  
92 trigger a thermodynamic forcing, which is of great importance for weather conditions  
93 in the surrounding regions (Bei et al., 2016; 2017; Zhao et al., 2015).

94

95 This study therefore focuses on how climate change on the Tibetan Plateau affects air  
96 quality in the Sichuan Basin in recent years. Section 3 analyzes the temperature change  
97 on the plateau in the past four decades, and especially emphasizes the change in recent  
98 five years. In Section 4, we design three sets of numerical simulations to calculate the  
99 impact of temperature change on air quality. One group includes two baseline  
100 simulations in two periods (January 2014 and January 2018), which are constrained by  
101 observed surface meteorological parameters and pollutant concentrations. The second  
102 group includes three sensitivity simulations during the 2013-2014 winter, which uses  
103 the same emission inventory and meteorological fields as the baseline simulation in  
104 January 2014 except for a changed air temperature. We also set the third sensitivity  
105 simulation, in which the plateau is also warming, but on the basis of the period for the  
106 2017-2018 winter. We compare the difference in PM<sub>2.5</sub> concentrations in these cases,

107 and also calculate differences in meteorological parameters that include winds (wind  
108 speed and direction), air temperature, and relative humidity (RH), as well as the  
109 Planetary Boundary Layer height (PBLH). Based on the differences in PM<sub>2.5</sub>  
110 concentration and meteorological parameters above, we finally explain the cause-to-  
111 effect relationship between a warming plateau and changes in the winds, PBLH and RH  
112 in the Sichuan Basin. Moreover, we calculate the effect of the relationship on air quality  
113 in the basin.

114

## 115 **2 Data and Methods**

116

### 117 **2.1 Observations**

118

119 To ensure a robust result, we use two datasets of surface air temperature in this study.  
120 One is the European Center for Medium-Range Weather Forecasts (ECMWF) ERA-  
121 Interim monthly mean reanalysis data (1979-2018), obtained from the website of  
122 <http://apps.ecmwf.int/datasets/>, with the finest horizontal resolution of 0.125°×0.125°.  
123 The other is hourly and monthly mean weather-station observations from the National  
124 Oceanic and Atmospheric Administration (NOAA), available from  
125 <http://gis.ncdc.noaa.gov/map/viewer/#app=clim&cfg=cdo&theme=hourly&layers=1>  
126  [&node=gis](http://gis.ncdc.noaa.gov/map/viewer/#app=clim&cfg=cdo&theme=hourly&layers=1).

127

128 Figure 1 shows the distribution of weather stations over the Tibetan Plateau, and these  
129 weather stations widely cover the entire plateau. Trends of annual mean and winter  
130 surface air temperature over the plateau are analyzed, and the winter is averaged over  
131 3-month periods (December-January-February). Additionally, we use ambient air  
132 quality data to validate the model performance. Since 2013, the data are released by  
133 Ministry of Environmental Protection, China at <http://www.aqjstudy.cn/>, including  
134 hourly PM<sub>2.5</sub>, CO, and O<sub>3</sub> mass concentrations. The monitoring stations for air quality

135 are also shown in Figure 1.

136

## 137 **2.2 Model configuration and experiments**

138

139 A state-of-the-art regional dynamical and chemical model (WRF-CHEM model) is  
140 used in the study. The simulation domain covers the Tibetan Plateau and the Sichuan  
141 Basin (Figure 1). The Tibetan Plateau covers about 2.5 million km<sup>2</sup>, with the averaged  
142 elevation of 4500 m, and the Sichuan Basin covers about 0.16 million km<sup>2</sup>, with the  
143 elevation in the center of the basin less than 1000 m (250 - 700 m). The model is set  
144 by a horizontal grid resolution of 9 km (451 × 221 grids), with 35 vertical sigma levels.  
145 The model description in detail is seen by Grell et al. (2005). The evaluation of the  
146 model performance has been conducted by many previous studies (Li et al., 2011a; Tie  
147 et al., 2009; 2007). In this study, we use the Goddard longwave and shortwave  
148 radiation parameterization (Dudhia, 1989), the WSM 6-class graupel microphysics  
149 scheme (Hong and Lim, 2006), the Mellor-Yamada-Janji (MYJ) planetary boundary  
150 layer scheme (Janjić, 2002), the unified Noah land-surface model (Chen and Dudhia,  
151 2001) and Monin-Obukhov surface layer scheme (Janjić, 2002). For chemical schemes,  
152 we use a new flexible gas-phase chemical module and the Community Multiscale Air  
153 Quality (CMAQ, version 4.6) aerosol module developed by the US EPA (Binkowski,  
154 2003). Gas-phase atmospheric reactions of volatile organic compounds (VOCs) and  
155 nitrogen oxide (NO<sub>x</sub>) use the SAPRC-99 (Statewide Air Pollution Research Center,  
156 version 1999) chemical mechanism. Inorganic aerosols use the ISORROPIA version  
157 1.7, referring to Li et al. (2011a) and Feng et al. (2016). A SO<sub>2</sub> heterogeneous reaction  
158 mechanism on aerosol surfaces involving aerosol water is added (Li et al., 2017a), and  
159 NO<sub>2</sub> heterogeneous reaction to produce HONO is also considered (Li et al., 2010). The  
160 secondary organic aerosol (SOA) calculation uses a non-traditional volatility basis-set  
161 approach by Li et al. (2011b). The photolysis rates are calculated by a fast Tropospheric  
162 Ultraviolet and Visible (FTUV) radiation transfer model, in which the impacts of

163 aerosols and clouds on the photochemistry processes are considered (Li et al., 2011a;  
164 Tie et al., 2003; 2005). The wet deposition is calculated by the method used in CMAQ  
165 and the dry deposition follows Wesely (1989).

166

167 We use the MIX anthropogenic emission inventory for the year of 2010, and it is  
168 available at Multi-resolution Emission Inventory for China  
169 (<http://www.meicmodel.org/dataset-mix.html>), consisting of industrial, power,  
170 transportation, and agricultural as well as residential sources (Li et al., 2017b; Zhang  
171 et al., 2009). The emission inventory is constructed by a ‘bottom-up’ approach based  
172 on national and provincial activity data and emission factors. To improve the emission  
173 inventory accuracy, we use a ‘top-down’ method here to constrain the emission  
174 inventory. We compare the simulated value with the measured value time and again  
175 until the simulations are close to the measurements. The biogenic emissions are online  
176 calculated by the Model of Emissions of Gases and Aerosol from Nature (MEGAN)  
177 (Guenther et al., 2006). Initial and boundary meteorological fields in the model are  
178 driven by 6-hour  $1^{\circ} \times 1^{\circ}$  NCEP (National Centers for Environmental Prediction)  
179 reanalysis data. Chemical lateral conditions are provided by a global chemistry  
180 transport model – MOZART (Model for OZone And Related chemical Tracer, version  
181 4), with a 6-h output (Emmons et al., 2010; Tie et al., 2005). The spin-up time of the  
182 WRF-CHEM model is 1 day.

183

184 According to the meteorological records at weather stations, surface air temperature  
185 risen by an average of  $2^{\circ}\text{C}$  from 2013 to 2017 over the plateau (Table S1). ERA-interim  
186 reanalysis data also show that the troposphere (600hPa - 250hPa) over the plateau is  
187 warming during the 2013-2017 period, and the temperature increment shows a  
188 parabolic pattern with the altitude, by an average increase of  $\sim 2^{\circ}\text{C}$  (Figure S1). Thus,  
189 we design several sensitivity simulations, with an average temperature increase in the  
190 troposphere over the plateau, to assess impacts of a warming plateau on air quality in

191 the basin. To eliminate the influence of simulation background, we conduct two  
192 baseline simulations for the 2013-2014 winter (January 2014) and the 2017-2018  
193 winter (January 2018) as the control groups. The other two sets focus on sensitivity  
194 simulations that reflect an observational increase in air temperature over the plateau.  
195 At the year of 2014, the sensitivity simulation uses the same emission inventory and  
196 meteorological conditions as the baseline simulation except that the temperature in the  
197 troposphere over the plateau respectively increases by 0.5°C, 1.0°C and 2.0°C. The  
198 third group is a sensitivity simulation with an increase of 2.0°C on the basis of air  
199 temperature in January 2018. In the domain, we set to the warming at all grids covering  
200 the plateau (the region surrounded by the dark line in Figure 1b) in the initial and  
201 boundary fields. In order to ensure a persistent influence of the warming, we drive the  
202 initial field with a 0.5°C, 1.0°C, and 2°C increment every day in January 2014, and a  
203 2°C increment every day in January 2018. Then, by comparing the difference between  
204 the sensitivity simulations and the baseline simulation, we determine the impact of the  
205 warming over the plateau on air quality in the basin.

206

### 207 **3 The warming Tibetan Plateau in the last four decades**

208

209 Figure 2 shows the variability and linear trend of surface air temperature at 10 weather  
210 stations over the Tibetan Plateau in winter during the last four decades (1979 - 2017).  
211 The winter mean temperature recorded from all the weather stations exhibits an  
212 obvious annual fluctuation and the linear regression shows a significant rising trend.  
213 Clearly, the plateau is continuously undergoing a warming phase, albeit with regional  
214 differences in the warming magnitude. The warming rates in different regions vary in  
215 the range of 0.5 - 1.0°C decade<sup>-1</sup>. Compared with the warming rate of annual mean  
216 temperature (Figure S2), the warming rate in winter is approximately twice as much,  
217 suggesting that the warming in winter is more significant.

218

219 Using the ERA-interim reanalysis data, Figure 3 shows the temperature change during  
220 the same period (1979 - 2017). The result is consistent with weather records, showing  
221 that air temperature is significantly rising in most parts of the plateau. The maximal  
222 warming rate is around 0.6 - 0.8°C decade<sup>-1</sup>, appeared in the central and southern  
223 plateau. The warming in the rest areas is slighter, with a rate of 0.3 - 0.6 °C decade<sup>-1</sup>.  
224 Particularly, the averaged warming rate in the vast central plateau reaches about 1.0°C  
225 yr<sup>-1</sup> in recent five years (Figure S3), greater than the warming rate during the entire 40  
226 years (Figure 3). Both the observation records and reanalysis data evidently show that  
227 the plateau has been warming in the last four decades, and also the warming trend for  
228 recent years is more significant.

229

230 From the above temperature change analysis, we notice that there is obviously a  
231 positive temperature anomaly between 2013 and 2017 winters, implying for an  
232 accelerating warming over the plateau. The observational temperature in winter  
233 increases by about 2°C between 2013 and 2017. **Therefore, we assess the impact of a**  
234 **warming plateau on air quality in the Sichuan Basin.**

235

## 236 **4 Results and Discussion**

237

### 238 **4.1 Model validation**

239

240 To systemically evaluate the model performance on simulation O<sub>3</sub>, CO and PM<sub>2.5</sub> mass  
241 concentrations, three statistical indices are used. They are the mean bias (MB), root  
242 mean square error (RMSE), and index of agreement (IOA). The calculation formulas  
243 are given in Text S1. The IOAs of air temperature and RH are 0.85 and 0.79,  
244 respectively (Figure S4a and Figure S4b), suggesting that the model well captures the  
245 diurnal cycle of temperature and the variability of RH. However, the calculated wind  
246 speed is overestimated, especially in the region between the Tibetan Plateau and the

247 Sichuan Basin. This is because there is a dramatic elevation drop in the region, which  
248 makes it difficult for the model to replicate the observed wind speed and direction.

249

250 Figure 4 shows comparisons of hourly  $O_3$ , CO and  $PM_{2.5}$  concentrations between the  
251 model simulations and measurements. The result shows that the simulated CO mean  
252 level is close to the measurement, with a MB of  $0.11 \text{ mg m}^{-3}$ , indicating that the model  
253 reasonably reproduces the meteorological fields and long-range transport. Because the  
254 chemical lifetime of CO is relatively long ( $\sim$ months), the variability of CO is  
255 dominantly determined by the meteorological fields and atmospheric transport process.  
256 For the simulation of  $O_3$ , in addition to the effects of meteorological fields and  
257 atmospheric transport process, its variability is strongly controlled by the  
258 photochemical process. The model result shows that the simulated diurnal cycle of  $O_3$   
259 is reasonably agreed with the measurement, with an IOA of 0.79. There is only a small  
260 bias between the simulated and measured  $O_3$  mean concentration. The simulated  $O_3$   
261 concentration is  $1.7 \text{ } \mu\text{g m}^{-3}$  higher than the measurement, suggesting that both the  
262 photochemistry and long-range transport well capture the  $O_3$  variability in the region.  
263 Finally, the IOA between the simulated and measured  $PM_{2.5}$  concentrations is 0.80,  
264 indicating that the aerosol module in the model generally captures the measured  $PM_{2.5}$   
265 variation.

266

267 However, there are some noticeable discrepancies between the simulations and the  
268 measurements. For instance, the simulated magnitude of  $PM_{2.5}$  concentration is larger  
269 than the measurement, and its mean level is underestimated by  $13.1 \text{ } \mu\text{g m}^{-3}$ , less than  
270 10% of the measurement ( $\sim 153.5 \text{ } \mu\text{g m}^{-3}$ ). These discrepancies are likely due to the  
271 biases in the uncertainties in emission inventory and small-scale dynamical fields.  
272 During the period of Jan 17<sup>th</sup> to Jan 20<sup>th</sup>, the observed wind speed concentrates in the  
273 range of  $1 - 2 \text{ m s}^{-1}$ , with an average of  $1.3 \text{ m s}^{-1}$ , while the simulated wind speed is  
274 obviously higher, with an average of  $2.0 \text{ m s}^{-1}$  (Figure S4c). The observed prevailing

275 wind is northerly wind while the simulated prevails easterly wind (Figure S4d). Figure  
276 S5a shows that PM<sub>2.5</sub> concentration is lower in the north to the Sichuan Basin while  
277 higher to in the east to the basin. Therefore, the overestimated PM<sub>2.5</sub> concentration is  
278 mainly caused by the departure of winds, which results in a false transport from the east  
279 to the basin. This is also shown by the overestimation of CO concentration because the  
280 observed northerly wind is not well simulated due to the complicated topography.

281

## 282 4.2 Change in winter PM<sub>2.5</sub> concentration over the basin

283

284 To examine impacts of a warming plateau on PM<sub>2.5</sub> concentration in winter in the basin,  
285 we set three levels of temperature increase of 0.5°C, 1.0°C and 2.0°C over the plateau.  
286 Time series of PM<sub>2.5</sub> concentrations in these simulations (with and without the  
287 warming over the plateau) are respectively calculated. The results show that PM<sub>2.5</sub>  
288 concentration in the basin is significantly reduced (Figure 5). In comparison with three  
289 levels of temperature increase, the maximal reduction occurs in the case of 2°C  
290 warming, with an average of 25.1 µg m<sup>-3</sup> ( $p < 0.001$ ). Under the circumstance of the  
291 2°C warming, the maximal hourly reduction reaches to 84.6 µg m<sup>-3</sup> (Figure S6a) and  
292 the maximal percentage reduction is about 64.4% (Figure S6b). We also calculate the  
293 changes in PM<sub>2.5</sub> concentration and its percentage under the influence of the 2°C  
294 warming on the basis of January 2018 (Figure S7), of which the result is consistent  
295 with Figure S6, though there must inevitably be some differences in the magnitude.  
296 Interestingly, the maximal reduction always occurs while PM<sub>2.5</sub> concentration reaches  
297 a peak value, which suggests that the impact of the warming plateau is extremely  
298 significant during the period of high PM<sub>2.5</sub> concentration. This result is similar to  
299 previous studies which also point out that extreme weather plays important roles in  
300 affecting air quality (De Sario et al., 2013; Hong et al., 2019; Tsangari et al., 2016;  
301 Zhang et al., 2016). That is to say, the impact of the warming plateau on air quality is  
302 apt to be amplified in extremely high PM<sub>2.5</sub> concentrations.

303

304 To better understand the impact of a warming plateau on PM<sub>2.5</sub> concentration, we also  
305 calculate changes in PM<sub>2.5</sub> chemical composition in the basin. Both primary and  
306 secondary aerosols in PM<sub>2.5</sub> decreases more significantly with an increase in  
307 temperature increment (Figure 6), except for the nitrate due to its competition for  
308 ammonia with sulfate (Feng et al., 2018). As a result, the more sulfate is reduced under  
309 the case of the 2°C warming, the less nitrate is reduced. As shown in Figure 6, the  
310 warmer the plateau is, the more PM<sub>2.5</sub> concentration and its chemical composition in  
311 the basin decrease, suggesting that a warming plateau has increasing implications for  
312 air quality in the basin. Here we show that the maximal impact of the plateau under  
313 the case of the 2°C warming, in which secondary aerosol reduces by 19.7 μg m<sup>-3</sup>,  
314 accounting for 78.5% of the total reduction, greatly larger than the reduction of primary  
315 aerosol. For example, the largest reduction is SOA, reducing from 23.2 μg m<sup>-3</sup> in the  
316 base case to 10.8 μg m<sup>-3</sup> in the 2°C warming case. The second reduction is sulfate  
317 (from 31.8 μg m<sup>-3</sup> to 28.6 μg m<sup>-3</sup>). The next are nitrate and ammonium (22.3 μg m<sup>-3</sup>  
318 and 19.1 μg m<sup>-3</sup> in the base case, and 20.2 μg m<sup>-3</sup> and 17.5 μg m<sup>-3</sup> in the 2°C warming  
319 case). Significance testing of the difference in every chemical composition between  
320 the baseline simulation and the 2°C warming case is also given in Table S2. The *p*-  
321 values of most chemical composition in PM<sub>2.5</sub> are far less than 0.001 except that the  
322 *p*-value of EC is 0.0011 (Table S2), implying for an extremely significant reduction of  
323 every chemical composition in PM<sub>2.5</sub> within the basin when the plateau warms by 2°C.  
324 Thus, we emphasize the impact of the 2°C warming over the plateau on PM<sub>2.5</sub>  
325 concentration in the basin in our study. Meanwhile, we analyze the case for the 2017-  
326 2018 winter, in which a similar change in PM<sub>2.5</sub> chemical composition is obtained  
327 when the plateau becomes 2°C warmer (Figure S8).

328

329 There are also significant changes in the spatial distribution of PM<sub>2.5</sub> concentration.  
330 Figure 7 shows the spatial distribution of changes in surface PM<sub>2.5</sub> concentration and

331 winds after 2°C warming over the plateau. Apparently, there is a larger decrease in  
332 PM<sub>2.5</sub> concentration in the whole basin, and the maximal reduction is more than 30 µg  
333 m<sup>-3</sup>. By contrast, PM<sub>2.5</sub> concentration increases by 5 - 15 µg m<sup>-3</sup> at the eastern edge of  
334 the plateau. Wind patterns show that easterly winds over the basin enhance while  
335 westerly wind over the plateau weaken (Figure S5 and Figure 7). Enhanced easterly  
336 winds and weakened westerly winds are both in favor of the east-to-west transport of  
337 pollutants from the basin to the plateau. We also show changes in PM<sub>2.5</sub> concentration  
338 and winds under the cases of 0.5°C and 1.0°C warming in January 2014, consistent  
339 with the result of the 2°C warming, except that the reduction of PM<sub>2.5</sub> concentration  
340 and the change in wind speed are fewer (Figure S9a and Figure S9e). The case in  
341 January 2018 (Figure S10a) is also similar to the result of the 2°C warming.

342

343 We further compare the difference in the surface pressure between the baseline and  
344 sensitivity simulations, and find out that surface pressure over the plateau and the basin  
345 all decreases when the plateau warms (Figure 8a and 8b). Over the plateau, the pressure  
346 drop has a decrease characteristic from west to east (Figure 8c, Figure S9b and Figure  
347 S9f, Figure S10b), which results in a decreased pressure gradient and a weakened  
348 westerly wind. While in the basin, the pressure drop is less than the plateau. This leads  
349 to an increased pressure gradient from the basin to the plateau, inducing an intensified  
350 easterly wind. The enhanced easterly wind causes an increased transport of PM<sub>2.5</sub> from  
351 the basin to the plateau. On the other hand, the weakened westerly wind and the  
352 enhanced easterly wind are convergent at the border between the plateau and the basin  
353 (Figure 7, Figure S9a and Figure S9e, Figure S10a), jointly leading to an increase in  
354 PM<sub>2.5</sub> concentration at the eastern edge of the plateau. Additionally, northerly winds  
355 over the basin slightly enhance, conducive to diluting the air and reducing PM<sub>2.5</sub>  
356 concentration. Both easterly winds transport and northerly winds dilution are favorable  
357 for a reduction of PM<sub>2.5</sub> concentration in the basin. In addition to the wind effect, there  
358 are also other important factors to produce the PM<sub>2.5</sub> reduction in the basin, such as the

359 **PBLH** and RH, which will be analyzed as follows.

360

### 361 **4.3 Impact of **PBLH** on **PM<sub>2.5</sub>** concentration**

362

363 Previous studies show that the PBL development plays an important role in diffusing  
364 pollutants (Miao et al., 2017; Su et al., 2018; Tie et al., 2015). Here we calculate the  
365 change in the **PBLH** due to the 2°C warming over the plateau, and then analyze the  
366 effect of the change in **PBLH** on **PM<sub>2.5</sub>** concentration in the basin.

367

368 Our results suggest that the warming plateau plays different roles in the PBL  
369 development over the plateau and the basin. Due to the warming, the PBLH decreases  
370 in most areas of the plateau, but it increases over the basin (Figure 9, Figure S9c and  
371 Figure S9g, Figure S10c). The maximal rise occurs under the case of the 2°C warming,  
372 by 50 - 200 m over the basin (Figure 9 and Figure S10c). As known, a shallow PBL  
373 constrains **PM<sub>2.5</sub>** near the surface via suppressing vertical dispersion (Fan et al., 2011;  
374 Iversen, 1984). Conversely, a deep PBL is favorable for **PM<sub>2.5</sub>** diffusion. Thus, we  
375 explore the underlying cause that leads to the difference in the PBLH in the domain.  
376 The PBLH is strongly related to the changes in vertical temperature and wind, Figure  
377 10 and Figures S11-12 display vertical profiles of changes in temperature and winds in  
378 the plateau and the basin. Results show that the warming causes a maximal warm layer  
379 around 1 km above the ground of the plateau. Noticeably, the warm layer acts as a dome  
380 covering 4.5 km above the Sichuan Basin (Figure 10a, Figure S11a and Figure S11c,  
381 Figure S12a). Xu et al. (2017) also finds out a significant warm plume extending from  
382 the plateau to the downstream Sichuan Basin and Yangtze River Delta by use of  
383 NCEP/NCAR reanalysis data. We suggest that this is probably due to a sharp  
384 topography decrease (from ~ 5 km in the plateau to < 1 km in the basin) which leads to  
385 a warm plume via subsidence. In the basin, there is a decrease in the temperature from  
386 the lower troposphere to ~ 4 km, with a maximal temperature reduction (0.5 - 2°C)

387 located at 1.5 km to 3 km above the ground (Figure 10a, Figure S11a and Figure S11c,  
388 Figure S12a). We speculate that changes in the surface pressure can account for the  
389 maximal temperature reduction here. After the warming, surface pressure decreases in  
390 the basin (Figure 8, Figure S9b and Figure S9f, Figure S10b), which produces more  
391 convergent airflow (as shown in Figure 7, Figure S9a and Figure S9e, Figure S10a).  
392 The strengthened convergent airflow induces an intensified ascending motion,  
393 conducive to a reduction of temperature in the basin. As a result, the zone where the  
394 maximal temperature drop appears, overlaps with the zone with the maximal ascending  
395 motion. Furthermore, the intensified updraft increases the vertical temperature gradient  
396 and the instability in the lower troposphere of the basin, thereby causing a higher PBLH  
397 than that in the non-warming case (Figure 10b, Figure S11b and Figure S11d, Figure  
398 S12b). On the contrary, the change in vertical temperature profile leads to a decreased  
399 vertical temperature gradient and increased thermal stability in the lower troposphere  
400 of the plateau, in which the PBLH decreases.

401

402 On the other hand, the convergent airflows by a weakened westerly wind over the  
403 plateau and a strengthened easterly wind in the basin triggers an ascending motion on  
404 the east side of the plateau (Figure 10a, Figure S11a and Figure S11c, Figure S12a),  
405 which is also beneficial to the development of the PBLH in the basin. Consequently,  
406 the elevated PBL facilitates vertical diffusion, leading to a reduction in  $PM_{2.5}$   
407 concentration over the basin.

408

#### 409 **4.4 Effect of RH on $PM_{2.5}$ concentration**

410

411 In addition to the PBLH, ambient RH is a key factor for secondary aerosol formation  
412 (Tie et al., 2017; Wang et al., 2016). Previous studies indicate that aerosol hygroscopic  
413 growth cannot occur until the humidity exceeds 50% (Liu et al., 2008). When the  
414 humidity is greater than 60%, hygroscopic growth factor of urban aerosol increases  
415 significantly with humidity (Liu et al., 2008).

416

417 We examine the influence of in the RH change induced by a warming plateau on PM<sub>2.5</sub>  
418 concentration in the basin. Results show that there is remarkable change in RH in the  
419 basin due to the warming of the plateau (Figure 11, Figure S9d and Figure S9h, Figure  
420 S10d). In the baseline simulation, the RH varies in the range of 40% - 80% over the  
421 basin (Figure 11a). However, the RH varies from 50% to 70% in the 2 °C warming  
422 simulation (Figure 11b), suggesting that the basin becomes drier when the plateau is  
423 warmer.

424

425 The RH comparison between these numerical simulations reveals that the warming  
426 causes a decrease in the RH within the basin (Figure 11c, Figure S9d and Figure S9h,  
427 Figure S10d). These changes in RH have critical effects on the secondary aerosol  
428 formation. As explained by Tie et al. (2017), the reduction of RH (especially during the  
429 stage of RH from 80% to 70%) causes a significant decrease of hygroscopic growth on  
430 the aerosol surface, resulting in less water surface for producing secondary aerosol,  
431 such as sulfate and nitrate. As a result, PM<sub>2.5</sub> concentration decreases in the basin. There  
432 are also some fingerprints of the RH's effect on PM<sub>2.5</sub> concentration. Firstly, the spatial  
433 distributions of RH reduction and PM<sub>2.5</sub> concentration reduction have similar patterns  
434 (Figure 11c and Figure 7, Figure S9a and Figure S9d, Figure S9e and Figure S9h, Figure  
435 S10a and Figure S10d), and the region with more humidity decrease overlaps the region  
436 with more PM<sub>2.5</sub> decreases. Secondly, as shown in Figure 6, the changes in PM<sub>2.5</sub>  
437 compositions indicate that the reduced PM<sub>2.5</sub> concentration is mainly caused by the  
438 decrease in secondary aerosol concentration. Therefore, the RH change also plays an  
439 important role for PM<sub>2.5</sub> concentration in the basin.

440

## 441 5 Conclusions

442

443 ERA-interim reanalysis data and observation records at 10 weather stations show that

444 the Tibetan Plateau is significantly warming during the past four decades (1979-2017),  
445 particularly in winter. The temperature increase rate is  $0.5^{\circ}\text{C decade}^{-1}$  to  $1.0^{\circ}\text{C decade}^{-1}$   
446 <sup>1</sup> in winter, approximately twice as much as the increase rate of annual mean  
447 temperature. In recent 5 years (2013-2017), the central plateau is significantly warming  
448 with an increase rate of  $1.0^{\circ}\text{C yr}^{-1}$ , encompassing the warming rate during the entire 40  
449 years. Rapid warming has caused the winter temperature to increase by an average of  
450  $2^{\circ}\text{C}$  over the entire plateau from 2013 to 2017.

451

452 The WRF-Chem model is used to assess the impact of a warming plateau on air quality  
453 over the downstream Sichuan Basin. The most significant impact of the plateau on  
454  $\text{PM}_{2.5}$  concentration in the basin occurs under the case of the  $2^{\circ}\text{C}$  warming. Through an  
455 enhanced horizontal transport, a reduced RH and an increased PBLH, the warming  
456 plateau significantly reduces  $\text{PM}_{2.5}$  concentration in the basin. A larger pressure  
457 gradient from the basin to the plateau is favorable for an east-to-west transport for  
458 pollutants within the basin. A lower ambient RH decreases aerosol hygroscopic growth,  
459 which weakens secondary aerosol formation and leads to a significant reduction in  
460 secondary aerosol concentration. Moreover, the warming induces an increase in vertical  
461 temperature gradient over the basin, strengthening turbulence mixing and elevating  
462 PBLH. The elevated PBLH is favorable for vertical diffusion that causes a reduction of  
463  $\text{PM}_{2.5}$  in the basin. Additionally, the uplift effect by an enhanced ascending motion at  
464 the eastern edge of the plateau also contributes to  $\text{PM}_{2.5}$  reduction within the basin.

465

466 In summary, the warming over the plateau in recent five years comprehensively induces  
467 a rising PBLH and a drying ambient air over the basin, which greatly reduces  $\text{PM}_{2.5}$   
468 secondary compositions. On average,  $\text{PM}_{2.5}$  concentration reduces by  $25.1 \mu\text{g m}^{-3}$  on  
469 the basis of the 2013-2014 winter, of which the primary and secondary aerosols  
470 decrease by  $5.4 \mu\text{g m}^{-3}$  and  $19.7 \mu\text{g m}^{-3}$ , respectively. Since the plateau is likely to  
471 continue warming, in-depth understanding to climate change on the Tibetan Plateau is

472 required. Long-term PM<sub>2.5</sub> monitoring is also needed to validate the impact of the  
473 warming plateau on air quality.

474

475 *Data availability.* The data used in this study are available from the corresponding  
476 author upon request (tiexx@ieecas.cn).

477 *Supplement.* Supplemental materials to this article can be found online at <http://xxxxxx>

478 *Author contributions.* XX designed research, and revised the final paper. SY performed  
479 research, and wrote the paper. XX and SY provided financial support. TF validated the  
480 model, modified the chart code and reviewed the paper. ZB collected and analyzed the  
481 weather-stations data.

482 *Competing interests.* The authors declare that they have no conflict of interest.

483 *Acknowledgements.* This work is supported by the National Natural Science Foundation  
484 of China (Nos. 41430424, 41730108 and 41807307) and the West Light Foundation of  
485 the Chinese Academy of Sciences (Nos. XAB2016B04). We also would like to  
486 acknowledge European Center for Medium-Range Weather Forecasts (ERA-interim)  
487 for reanalysis data which are freely obtained by a following registration on the website  
488 <http://apps.ecmwf.int/datasets/>. Ambient weather-station observations are obtained  
489 from the National Oceanic and Atmospheric Administration (NOAA),  
490 <http://gis.ncdc.noaa.gov/map/viewer/#app=clim&cfg=cdo&theme=hourly&layers=1>  
491 &node=gis. The hourly ambient surface O<sub>3</sub>, CO and PM<sub>2.5</sub> mass concentrations are real-  
492 timely released by Ministry of Environmental Protection, China on the website  
493 <http://www.aqistudy.cn/>, freely downloaded from <http://106.37.208.233:20035/>. The  
494 MEIC-2012 (Multi-resolution Emission Inventory for China) anthropogenic emission  
495 inventory is available on the website, <http://www.meicmodel.org>. The authors also  
496 thank anonymous reviewers for their helpful comments and suggestions.

## 497 **Reference**

498

499 Bei, N., Li, G., Huang, R.-J., Cao, J., Meng, N., Feng, T., Liu, S., Zhang, T., Zhang, Q. and Molina,  
500 L. T.: Typical synoptic situations and their impacts on the wintertime air pollution in the Guanzhong  
501 basin, China, *Atmos. Chem. Phys.*, 16(11), 7373–7387, doi:10.5194/acp-16-7373-2016, 2016.

502 Bei, N., Zhao, L., Xiao, B., Meng, N. and Feng, T.: Impacts of local circulations on the wintertime  
503 air pollution in the Guanzhong Basin, China, *Science of The Total Environment*, 592, 373–390,  
504 doi:10.1016/j.scitotenv.2017.02.151, 2017.

505 Binkowski, F. S.: Models-3 Community Multiscale Air Quality (CMAQ) model aerosol component  
506 1. Model description, *J. Geophys. Res.*, 108(D6), 2981, doi:10.1029/2001JD001409, 2003.

507 Cai, W., Li, K., Liao, H., Wang, H. and Wu, L.: Weather conditions conducive to Beijing severe  
508 haze more frequent under climate change, *Nat. Clim. Change*, 7(4), 257–262,  
509 doi:10.1038/nclimate3249, 2017.

510 Chen, F. and Dudhia, J.: Coupling an Advanced Land Surface–Hydrology Model with the Penn  
511 State–NCAR MM5 Modeling System. Part I: Model Implementation and Sensitivity, *Mon. Weather*  
512 *Rev.*, 129(4), 569–585, doi:10.1175/1520-0493(2001)129<0569:CAALSH>2.0.CO;2, 2001.

513 De Sario, M., Katsouyanni, K. and Michelozzi, P.: Climate change, extreme weather events, air  
514 pollution and respiratory health in Europe, *Eur Respir J*, 42(3), 826–843,  
515 doi:10.1183/09031936.00074712, 2013.

516 Duan, A., Wu, G., Liu, Y., Ma, Y. and Zhao, P.: Weather and climate effects of the Tibetan Plateau,  
517 *Adv. in Atmos. Sci.*, 29(5), 978–992, doi:10.1007/s00376-012-1220-y, 2012.

518 Dudhia, J.: Numerical Study of Convection Observed during the Winter Monsoon Experiment  
519 Using a Mesoscale Two-Dimensional Model, *J. Atmos. Sci.*, 46(20), 3077–3107, doi:10.1175/1520-  
520 0469(1989)046<3077:NSOCOD>2.0.CO;2, 1989.

521 Emmons, L. K., Walters, S., Hess, P. G., Lamarque, J. F., Pfister, G. G., Fillmore, D., Granier, C.,  
522 Guenther, A., Kinnison, D., Laepple, T., Orlando, J., Tie, X., Tyndall, G., Wiedinmyer, C.,  
523 Baughcum, S. L. and Kloster, S.: Description and evaluation of the Model for Ozone and Related  
524 chemical Tracers, version 4 (MOZART-4), *Geosci. Model Dev.*, 3(1), 43–67, doi:10.5194/gmd-3-  
525 43-2010, 2010.

526 Fan, S. J., Fan, Q., Yu, W., Luo, X. Y., Wang, B. M., Song, L. L. and Leong, K. L.: Atmospheric  
527 boundary layer characteristics over the Pearl River Delta, China, during the summer of 2006:  
528 measurement and model results, *Atmos. Chem. Phys.*, 11(13), 6297–6310, doi:10.5194/acp-11-  
529 6297-2011, 2011.

530 Feng, T., Bei, N., Zhao, S., Wu, J., Li, X., Zhang, T., Cao, J., Zhou, W. and Li, G.: Wintertime nitrate  
531 formation during haze days in the Guanzhong basin, China: A case study, *Environmental Pollution*,  
532 243(Part B), 1057–1067, doi:10.1016/j.envpol.2018.09.069, 2018.

533 Feng, T., Li, G., Cao, J., Bei, N., Shen, Z., Zhou, W., Liu, S., Zhang, T., Wang, Y., Huang, R.-J., Tie,  
534 X. and Molina, L. T.: Simulations of organic aerosol concentrations during springtime in the  
535 Guanzhong Basin, China, *Atmos. Chem. Phys.*, 16(15), 10045–10061, doi:10.5194/acp-16-10045-  
536 2016, 2016.

537 Grell, G. A., Peckham, S. E., Schmitz, R., McKeen, S. A., Frost, G., Skamarock, W. C. and Eder,  
538 B.: Fully coupled “online” chemistry within the WRF model, *Atmos. Environ.*, 39(37), 6957–6975,  
539 doi:10.1016/j.atmosenv.2005.04.027, 2005.

540 Guenther, A., Karl, T., Harley, P., Wiedinmyer, C., Palmer, P. I. and Geron, C.: Estimates of global  
541 terrestrial isoprene emissions using MEGAN (Model of Emissions of Gases and Aerosols from  
542 Nature), *Atmos. Chem. Phys.*, 6(11), 3181–3210, doi:10.5194/acp-6-3181-2006, 2006.

543 Hong, C., Zhang, Q., Zhang, Y., Davis, S. J., Tong, D., Zheng, Y., Liu, Z., Guan, D., He, K. and  
544 Schellnhuber, H. J.: Impacts of climate change on future air quality and human health in China, *P.*  
545 *Natl. Acad. Sci. USA*, 116(35), 17193–17200, doi:10.1073/pnas.1812881116, 2019.

546 Hong, S.-Y. and Lim, J.-O. J.: The WRF single-moment 6-class microphysics scheme (WSM6), *J.*  
547 *Korean Meteor. Soc.*, 42(2), 129–151, 2006.

548 Hua, M.: Analysis and simulation study on the influence of heat condition over Qinghai-Xizang  
549 Plateau on climate over South-West China, *Plateau Meteorology*, 22, 152–156, 2017.

550 Iversen, T.: On the atmospheric transport of pollution to the Arctic, *Geophys. Res. Lett.*, 11(5), 457–  
551 460, doi:10.1029/GL011i005p00457, 1984.

552 Janjić, Z. I.: Nonsingular implementation of the Mellor-Yamada level 2.5 scheme in the NCEP meso  
553 model, Camp Springs, MD. 2002.

554 Kuang, X. and Jiao, J. J.: Review on climate change on the Tibetan Plateau during the last half  
555 century, *J. Geophys. Res.*, 1–29, doi:10.1002/(ISSN)2169-8996, 2016.

556 Li, G., Bei, N., Cao, J., Huang, R., Wu, J., Feng, T., Wang, Y., Liu, S., Zhang, Q., Tie, X. and Molina,  
557 L. T.: A possible pathway for rapid growth of sulfate during haze days in China, *Atmos. Chem. Phys.*,  
558 17(5), 3301–3316, doi:10.5194/acp-17-3301-2017, 2017a.

559 Li, G., Bei, N., Tie, X. and Molina, L. T.: Aerosol effects on the photochemistry in Mexico City  
560 during MCMA-2006/MILAGRO campaign, *Atmos. Chem. Phys.*, 11(11), 5169–5182,  
561 doi:10.5194/acp-11-5169-2011, 2011a.

562 Li, G., Lei, W., Zavala, M., Volkamer, R., Dusanter, S., Stevens, P. and Molina, L. T.: Impacts of  
563 HONO sources on the photochemistry in Mexico City during the MCMA-2006/MILAGO  
564 Campaign, *Atmos. Chem. Phys.*, 10(14), 6551–6567, doi:10.5194/acp-10-6551-2010, 2010.

565 Li, G., Zavala, M., Lei, W., Tsimpidi, A. P., Karydis, V. A., Pandis, S. N., Canagaratna, M. R. and  
566 Molina, L. T.: Simulations of organic aerosol concentrations in Mexico City using the WRF-CHEM  
567 model during the MCMA-2006/MILAGRO campaign, *Atmos. Chem. Phys.*, 11(8), 3789–3809,  
568 doi:10.5194/acp-11-3789-2011, 2011b.

569 Li, M., Zhang, Q., Kurokawa, J.-I., Woo, J.-H., He, K., Lu, Z., Ohara, T., Song, Y., Streets, D. G.,  
570 Carmichael, G. R., Cheng, Y., Hong, C., Huo, H., Jiang, X., Kang, S., Liu, F., Su, H. and Zheng, B.:  
571 MIX: a mosaic Asian anthropogenic emission inventory under the international collaboration  
572 framework of the MICS-Asia and HTAP, *Atmos. Chem. Phys.*, 17(2), 935–963, doi:10.5194/acp-  
573 17-935-2017, 2017b.

574 Liu, X. and Chen, B.: CLIMATIC WARMING IN THE TIBETAN PLATEAU DURING RECENT  
575 DECADES, *Int. J. Climatol.*, 20, 1729–1742, 2000.

576 Liu, X., Cheng, Y., Zhang, Y., Jung, J., Sugimoto, N., Chang, S.-Y., Kim, Y. J., Fan, S. and Zeng, L.:  
577 Influences of relative humidity and particle chemical composition on aerosol scattering properties  
578 during the 2006 PRD campaign, *Atmos. Environ.*, 42(7), 1525–1536,  
579 doi:10.1016/j.atmosenv.2007.10.077, 2008.

580 Miao, Y., Guo, J., Liu, S., Liu, H., Li, Z., Zhang, W. and Zhai, P.: Classification of summertime  
581 synoptic patterns in Beijing and their associations with boundary layer structure affecting aerosol  
582 pollution, *Atmos. Chem. Phys.*, 17(4), 3097–3110, doi:10.5194/acp-17-3097-2017, 2017.

583 Qiao, X., Guo, H., Tang, Y., Wang, P., Deng, W., Zhao, X., Hu, J., Ying, Q. and Zhang, H.: Local  
584 and regional contributions to fine particulate matter in the 18 cities of Sichuan Basin, southwestern  
585 China, *Atmos. Chem. Phys.*, 19(9), 5791–5803, doi:10.5194/acp-19-5791-2019, 2019.

586 Rangwala, I., Miller, J. R. and Xu, M.: Warming in the Tibetan Plateau: Possible influences of the  
587 changes in surface water vapor, *Geophys. Res. Lett.*, 36(6), 5–6, doi:10.1029/2009GL037245, 2009.

588 Su, T., Li, Z. and Kahn, R.: Relationships between the planetary boundary layer height and surface  
589 pollutants derived from lidar observations over China: regional pattern and influencing factors,  
590 *Atmos. Chem. Phys.*, 18(21), 15921–15935, doi:10.5194/acp-18-15921-2018, 2018.

591 Tao, J., Zhang, L., Cao, J. and Zhang, R.: A review of current knowledge concerning PM  
592 2.5 chemical composition, aerosol optical properties and their relationships across China, *Atmos.*  
593 *Chem. Phys.*, 17(15), 9485–9518, doi:10.5194/acp-17-9485-2017, 2017.

594 Tie, X., Huang, R.-J., Cao, J., Zhang, Q., Cheng, Y., Su, H., Di Chang, schl, U. P. X., Hoffmann, T.,  
595 Dusek, U., Li, G., Worsnop, D. R. and Dowd, C. D. O. X.: Severe Pollution in China Amplified by  
596 Atmospheric Moisture, *Sci. Rep.*, 1–8, doi:10.1038/s41598-017-15909-1, 2017.

597 Tie, X., Madronich, S., Li, G., Ying, Z., Weinheimer, A., Apel, E. and Campos, T.: Simulation of  
598 Mexico City plumes during the MIRAGE-Mex field campaign using the WRF-Chem model, *Atmos.*  
599 *Chem. Phys.*, 9(14), 4621–4638, doi:10.5194/acp-9-4621-2009, 2009.

600 Tie, X., Madronich, S., Li, G., Ying, Z., Zhang, R., Garcia, A. R., Lee-Taylor, J. and Liu, Y.:  
601 Characterizations of chemical oxidants in Mexico City: A regional chemical dynamical model  
602 (WRF-Chem) study, *Atmos. Environ.*, 41(9), 1989–2008, doi:10.1016/j.atmosenv.2006.10.053,  
603 2007.

604 Tie, X., Madronich, S., Walters, S., Zhang, R., Rasch, P. and Collins, W.: Effect of clouds on  
605 photolysis and oxidants in the troposphere, *J. Geophys. Res.*, 108(D20), 4642,  
606 doi:10.1029/2003JD003659, 2003.

607 Tie, X., Sasha, M., Stacy, W., David, E., Paul, G., Natalie, M., Renyi, Z., Lou, C. and Guy, B.:

608 Assessment of the global impact of aerosols on tropospheric oxidants, *J. Geophys. Res.*,  
609 110(D03204), 13,791, doi:10.1029/2004JD005359, 2005.

610 Tie, X., Zhang, Q., He, H., Cao, J., Han, S., Gao, Y., Li, X. and Jia, X. C.: A budget analysis of the  
611 formation of haze in Beijing, *Atmos. Environ.*, 100, 25–36, doi:10.1016/j.atmosenv.2014.10.038,  
612 2015.

613 Tsangari, H., Paschalidou, A. K., Kassomenos, A. P., Vardoulakis, S., Heaviside, C., Georgiou, K.  
614 E. and Yamasaki, E. N.: Extreme weather and air pollution effects on cardiovascular and respiratory  
615 hospital admissions in Cyprus, *Science of The Total Environment*, 542(Part A), 247–253,  
616 doi:10.1016/j.scitotenv.2015.10.106, 2016.

617 Wang, G., Zhang, R., Gomez, M. E., Yang, L., Levy Zamora, M., Hu, M., Lin, Y., Peng, J., Guo, S.,  
618 Meng, J., Li, J., Cheng, C., Hu, T., Ren, Y., Wang, Y., Gao, J., Cao, J., An, Z., Zhou, W., Li, G.,  
619 Wang, J., Tian, P., Marrero-Ortiz, W., Secret, J., Du, Z., Zheng, J., Shang, D., Zeng, L., Shao, M.,  
620 Wang, W., Huang, Y., Wang, Y., Zhu, Y., Li, Y., Hu, J., Pan, B., Cai, L., Cheng, Y., Ji, Y., Zhang, F.,  
621 Rosenfeld, D., Liss, P. S., Duce, R. A., Kolb, C. E. and Molina, M. J.: Persistent sulfate formation  
622 from London Fog to Chinese haze, *P. Natl. Acad. Sci. USA*, 113(48), 13630–13635,  
623 doi:10.1073/pnas.1616540113, 2016.

624 Wang, H., Tian, M., Chen, Y., Shi, G., Liu, Y., Yang, F., Zhang, L., Deng, L., Yu, J., Peng, C. and  
625 Cao, X.: Seasonal characteristics, formation mechanisms and source origins of PM<sub>2.5</sub> in two  
626 megacities in Sichuan Basin, China, *Atmos. Chem. Phys.*, 18(2), 865–881, doi:10.5194/acp-18-865-  
627 2018, 2018.

628 Wesely, M. L.: Parameterization of surface resistances to gaseous dry deposition in regional-scale  
629 numerical models, *Atmospheric Environment* (1967), 23(6), 1293–1304, doi:10.1016/0004-  
630 6981(89)90153-4, 1989.

631 Xu, J., Chang, L., Yan, F. and He, J.: Role of climate anomalies on decadal variation in the  
632 occurrence of wintertime haze in the Yangtze River Delta, China, *Science of The Total Environment*,  
633 599-600, 918–925, doi:10.1016/j.scitotenv.2017.05.015, 2017.

634 Xu, X., Zhao, T., Liu, F., Gong, S. L., Kristovich, D., Lu, C., Guo, Y., Cheng, X., Wang, Y. and Ding,  
635 G.: Climate modulation of the Tibetan Plateau on haze in China, *Atmos. Chem. Phys.*, 16(3), 1365–  
636 1375, doi:10.5194/acp-16-1365-2016, 2016.

637 Yang, F., Tan, J., Zhao, Q., Du, Z., He, K., Ma, Y., Duan, F., Chen, G. and Zhao, Q.: Characteristics  
638 of PM<sub>2.5</sub>speciation in representative megacities and across China, *Atmos. Chem. Phys.*, 11(11),  
639 5207–5219, doi:10.5194/acp-11-5207-2011, 2011.

640 Zhang, H., Wang, Y., Park, T.-W. and Deng, Y.: Quantifying the relationship between extreme air  
641 pollution events and extreme weather events, *Atmospheric Research*, 1–48,  
642 doi:10.1016/j.atmosres.2016.11.010, 2016.

643 Zhang, Q., Streets, D. G., Carmichael, G. R., He, K. B., Huo, H., Kannari, A., Klimont, Z., Park, I.  
644 S., Reddy, S., Fu, J. S., Chen, D., Duan, L., Lei, Y., Wang, L. T. and Yao, Z. L.: Asian emissions in  
645 2006 for the NASA INTEX-B mission, *Atmos. Chem. Phys.*, 9(14), 5131–5153, doi:10.5194/acp-  
646 9-5131-2009, 2009.

647 Zhao, P., Li, Y., Guo, X., Xu, X., Liu, Y., Tang, S., Xiao, W., Shi, C., Ma, Y., Yu, X., Liu, H., Jia, L.,  
648 Chen, Y., Liu, Y., Li, J., Luo, D., Cao, Y., Zheng, X., Chen, J., Xiao, A., Yuan, F., Chen, D., Pang,  
649 Y., Hu, Z., Zhang, S., Dong, L., Hu, J., Han, S. and Zhou, X.: The Tibetan Plateau Surface-  
650 Atmosphere Coupling System and Its Weather and Climate Effects: The Third Tibetan Plateau  
651 Atmospheric Science Experiment, *J Meteorol Res*, 33(3), 375–399, doi:10.1007/s13351-019-8602-  
652 3, 2019.

653 Zhao, S., Feng, T., Tie, X., Long, X., Li, G., Cao, J., Zhou, W. and An, Z.: Impact of Climate Change  
654 on Siberian High and Wintertime Air Pollution in China in Past Two Decades, *Earth's Future*, 6,  
655 118–133, doi:10.1002/2017EF000682, 2018.

656 Zhao, S., Tie, X., Cao, J. and Zhang, Q.: Impacts of mountains on black carbon aerosol under  
657 different synoptic meteorology conditions in the Guanzhong region, China, *Atmospheric Research*,  
658 164-165(C), 286–296, doi:10.1016/j.atmosres.2015.05.016, 2015.

659 Zhu, Q., Shou, S. and Tang, D.: Principles and methods of weather, 4 ed., Beijing, 2000.

660 Zou, Y., Wang, Y., Zhang, Y. and Koo, J.-H.: Arctic sea ice, Eurasia snow, and extreme winter haze  
661 in China, *Sci. Adv.*, 3(3), e1602751–9, doi:10.1126/sciadv.1602751, 2017.

662

## Figure captions

663

664

665 **Figure 1** (a) Location map of the Tibetan Plateau (the region surrounded by the dark line) and  
666 the Sichuan Basin (the region surrounded by the gray line). (b) The model domain and  
667 the distribution of weather stations marked in the triangles over the Tibetan Plateau  
668 and air quality stations marked in the circles over the Sichuan Basin.

669 **Figure 2** Trends of observational winter (Dec-Jan-Feb) mean temperature anomaly recorded  
670 by 10 weather stations over the Tibetan Plateau during the last four decades (1979-  
671 2017).

672 **Figure 3** Trends of ERA-interim reanalysis winter mean temperature over the Tibetan Plateau  
673 from 1979 to 2017. The dotted regions show statistical significance with 95%  
674 confidence level ( $p$ -value  $< 0.05$ ) from the Student's  $t$  test.

675 **Figure 4** Comparison between the observed (black dots) and simulated (blue line) hourly  $O_3$   
676 ( $\mu\text{g m}^{-3}$ ), CO ( $\text{mg m}^{-3}$ ) and  $\text{PM}_{2.5}$  mass concentration ( $\mu\text{g m}^{-3}$ ) over the Sichuan Basin  
677 in January 2014.

678 **Figure 5** Time series of  $\text{PM}_{2.5}$  concentration over the Sichuan Basin, the baseline simulation is  
679 selected in January 2014 and the sensitivity simulations in which  $0.5^\circ\text{C}$ ,  $1.0^\circ\text{C}$ , and  
680  $2^\circ\text{C}$  warming occur over the Tibetan Plateau relative to the baseline simulation. The  
681 differences in  $\text{PM}_{2.5}$  concentrations between the baseline simulation and sensitivity  
682 simulations are significant, exceeding 99.9% confidence level ( $p < 0.001$ ).

683 **Figure 6** Comparisons of  $\text{PM}_{2.5}$  chemical composition in the Sichuan Basin between the  
684 baseline simulation (black) and sensitivity simulations that the plateau warms by  $0.5^\circ\text{C}$   
685 ( $0.5^\circ\text{C}$  (green),  $1.0^\circ\text{C}$  (yellow) and  $2.0^\circ\text{C}$  (red)).

686 **Figure 7** Difference in spatial distributions of surface  $\text{PM}_{2.5}$  concentration (shading) and winds  
687 (arrows) between the sensitivity simulation and baseline simulation. The negative  
688 shows  $\text{PM}_{2.5}$  concentration decreases and the positive shows  $\text{PM}_{2.5}$  concentration  
689 increases when the Tibetan Plateau is  $2^\circ\text{C}$  warming.

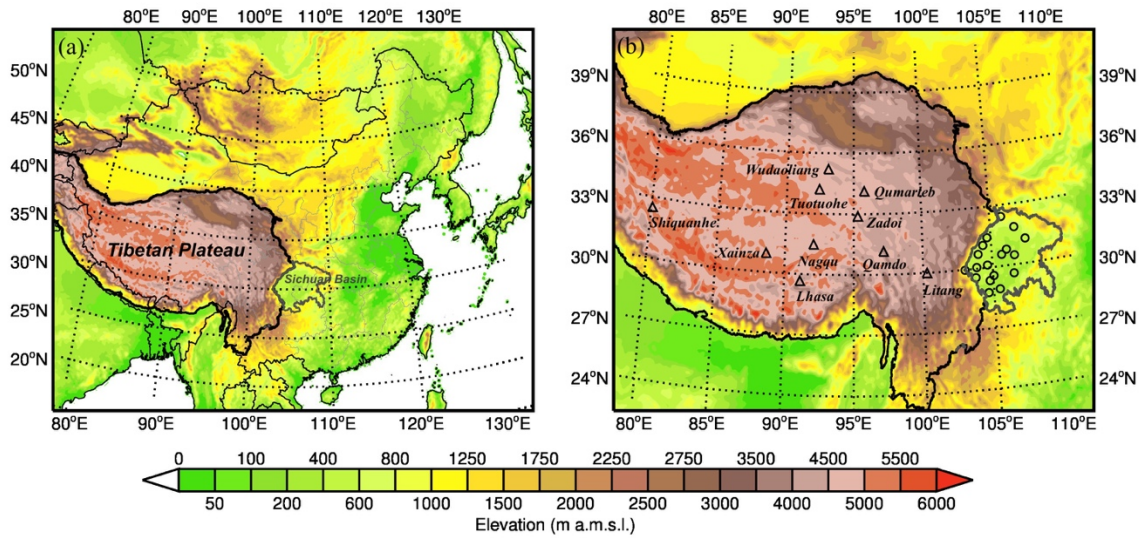
690 **Figure 8** Comparison of spatial distributions of sea level pressure (SLP) between the (a)  
691 baseline simulation and (b) sensitivity simulation over the Tibetan Plateau and Sichuan  
692 Basin. (c) Changes in SLPs (sensitivity simulation *minus* baseline simulation) over the  
693 plateau and basin while the plateau becomes  $2^\circ\text{C}$  warming.

694 **Figure 9** Spatial change in the PBLH induced by  $2^\circ\text{C}$  warming over the Tibetan Plateau. The  
695 positive shows the PBLH increases while the negative shows the PBLH decreases.

696 **Figure 10** Vertical profiles of changes in temperature (shading and gray contour) and winds  
697 (arrows) along  $30^\circ\text{N}$  in January 2014. The gray shaded area presents topography. The  
698 green box for the Sichuan Basin, and the red solid (baseline simulation) and dash  
699 (sensitivity simulation) lines for the PBLH. (a) The Tibetan Plateau and Sichuan Basin,  
700 and (b) The Sichuan Basin.

701 **Figure 11** Comparison of spatial distributions of RH between (a) baseline simulation and (b)  
702 sensitivity simulation over the Tibetan Plateau and Sichuan Basin. (c) Similar to Figure  
703 9, but for RH spatial changes when the plateau becomes  $2^\circ\text{C}$  warming, and the positive  
704 shows the RH increases while the negative shows the RH decreases.

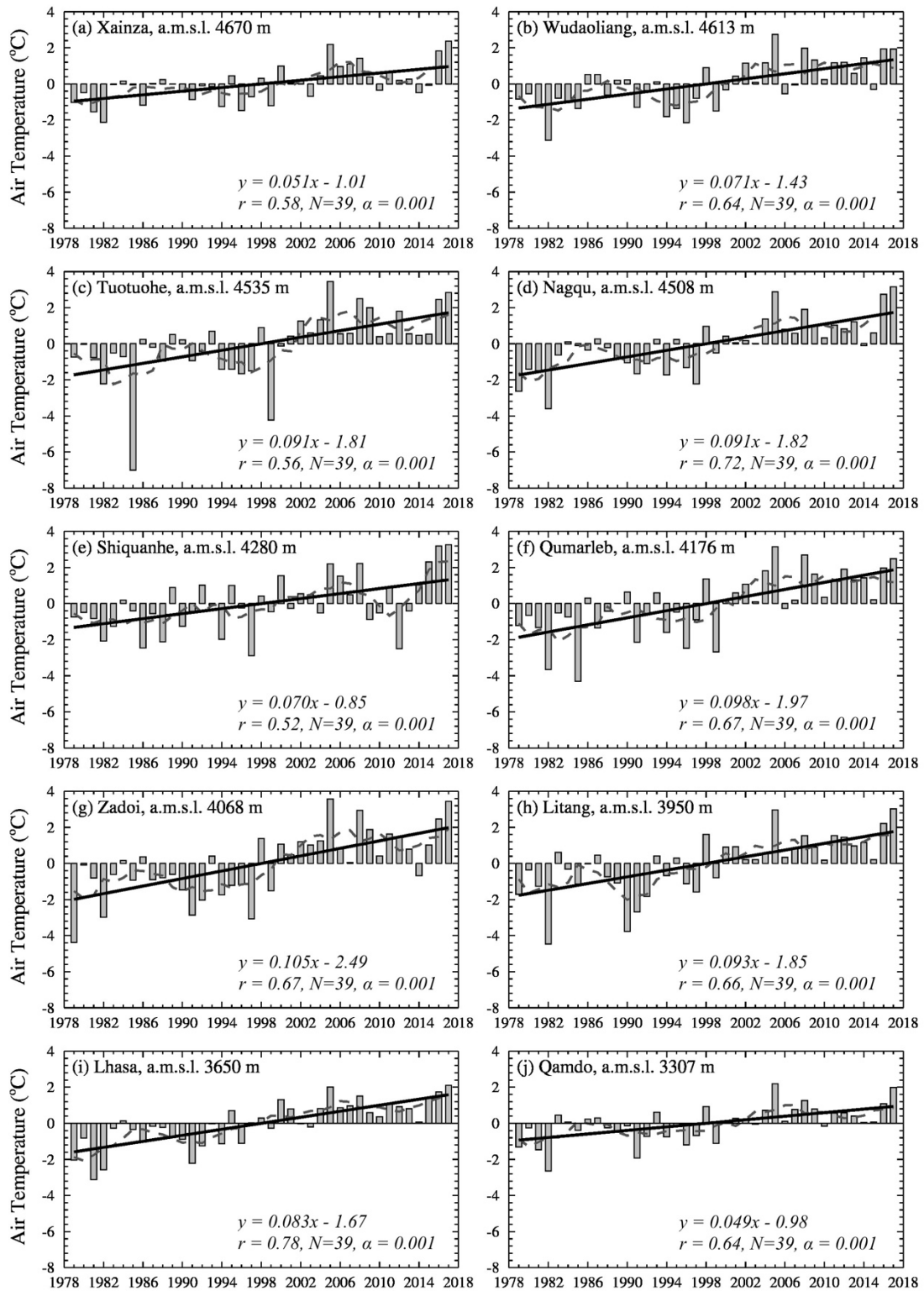
705



707

708 **Figure 1** (a) Location map of the Tibetan Plateau (the region surrounded by the dark line) and  
 709 the Sichuan Basin (the region surrounded by the gray line). (b) The model domain and the  
 710 distribution of weather stations marked in the triangles over the Tibetan Plateau and air quality  
 711 stations marked in the circles over the Sichuan Basin.

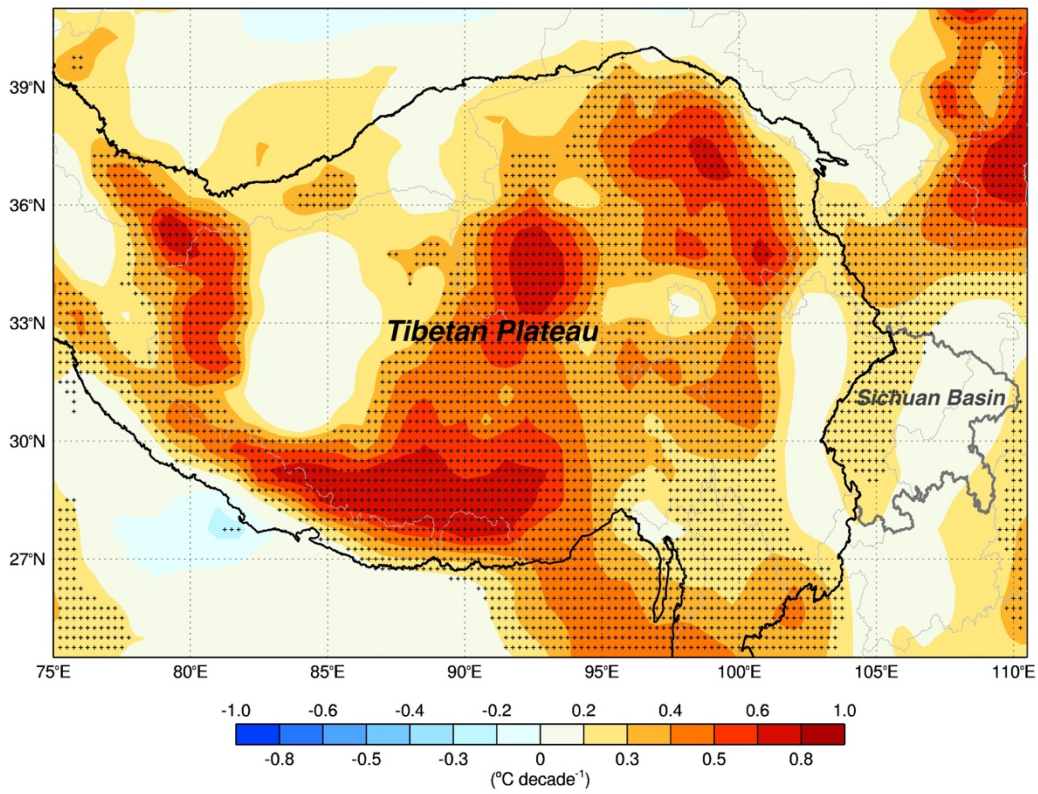
712



713

714 **Figure 2** Trends of observational winter (Dec-Jan-Feb) mean temperature anomaly recorded  
 715 by 10 weather stations over the Tibetan Plateau during the last four decades (1979-2017).

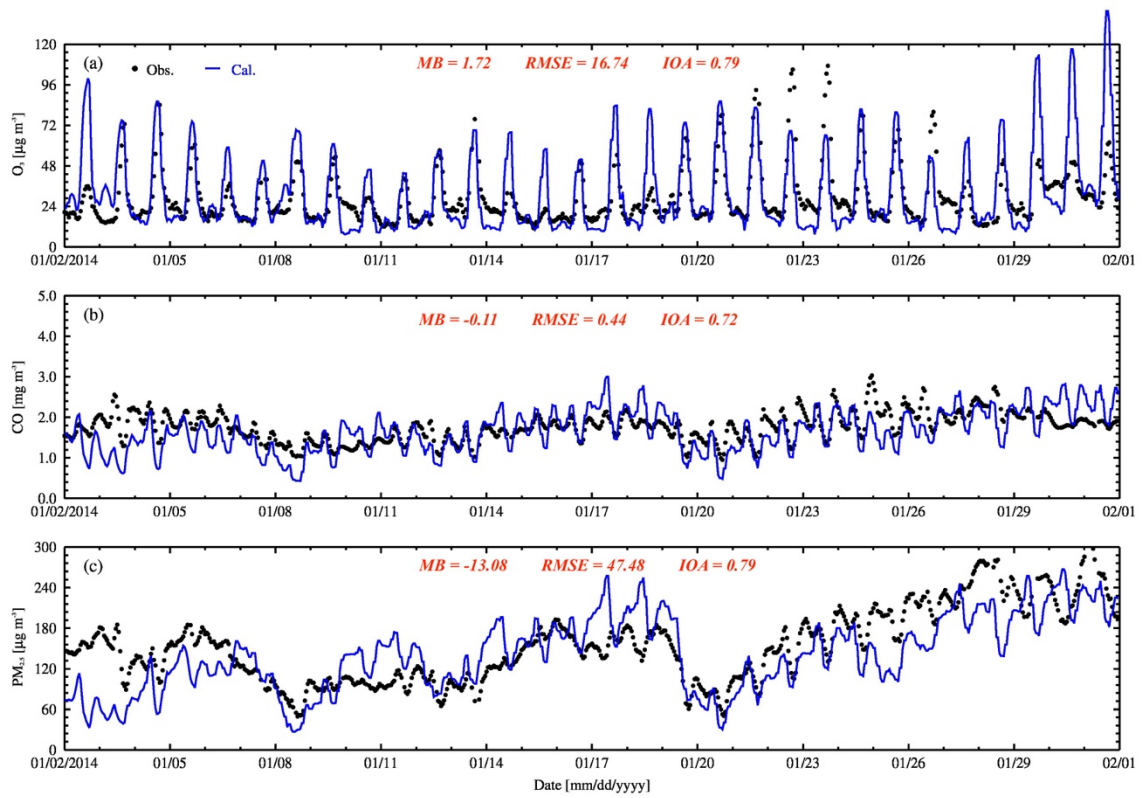
716



718

719 **Figure 3** Trends of ERA-interim reanalysis winter mean temperature over the Tibetan Plateau  
 720 from 1979 to 2017. The dotted regions show statistical significance with 95% confidence level  
 721 ( $p$ -value < 0.05) from the Student's  $t$  test.

722

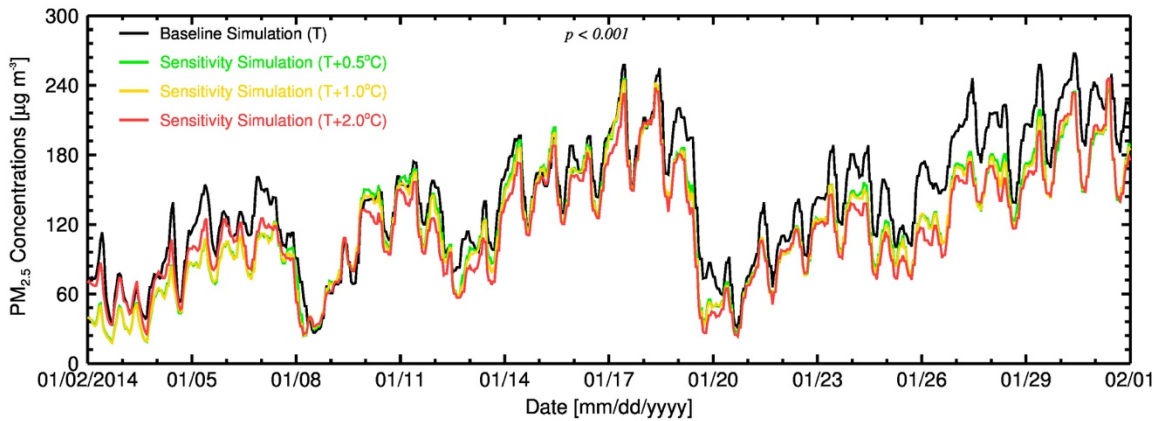


724

725 **Figure 4** Comparison between the observed (black dots) and simulated (blue line) hourly  $O_3$   
 726 ( $\mu\text{g m}^{-3}$ ),  $\text{CO}$  ( $\text{mg m}^{-3}$ ) and  $\text{PM}_{2.5}$  mass concentration ( $\mu\text{g m}^{-3}$ ) over the Sichuan Basin in  
 727 January 2014.

728

729



730

731

732

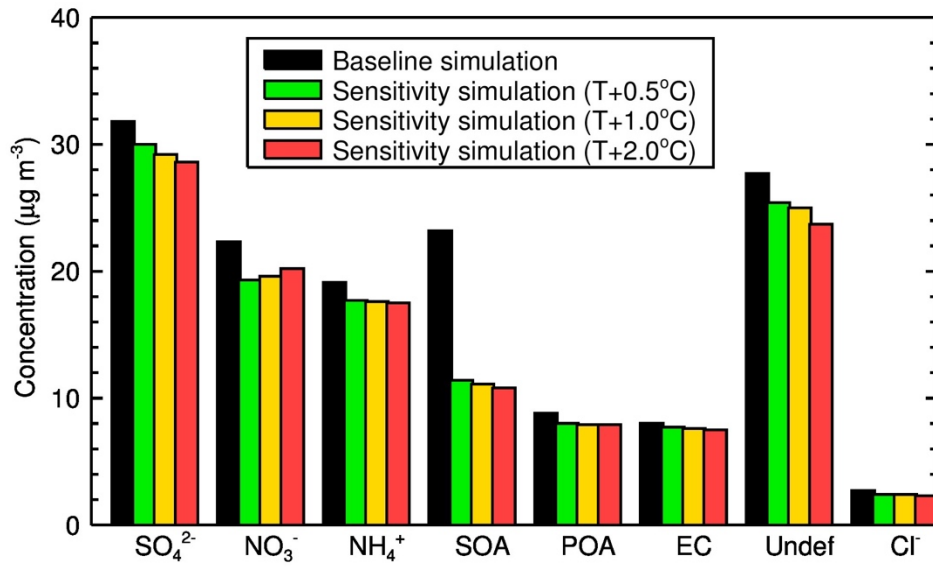
733

734

735

736

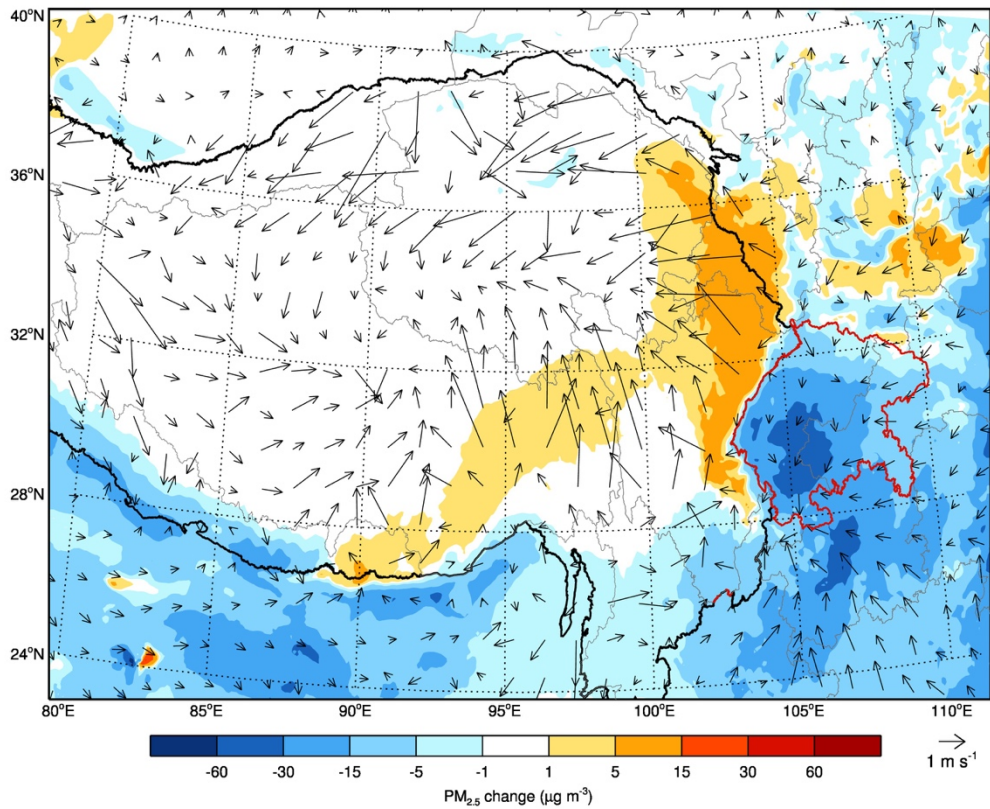
**Figure 5** Time series of PM<sub>2.5</sub> concentration over the Sichuan Basin, the baseline simulation is selected in January 2014 and the sensitivity simulations in which 0.5°C, 1.0°C, and 2°C warming occur over the Tibetan Plateau relative to the baseline simulation. The differences in PM<sub>2.5</sub> concentrations between the baseline simulation and sensitivity simulations are significant, exceeding 99.9% confidence level ( $p < 0.001$ ).



738

739 **Figure 6** Comparisons of PM<sub>2.5</sub> chemical composition in the Sichuan Basin between the  
 740 baseline simulation (black) and sensitivity simulations that the plateau warms by 0.5°C (green),  
 741 1.0°C (yellow) and 2.0°C (red).

742



744

745

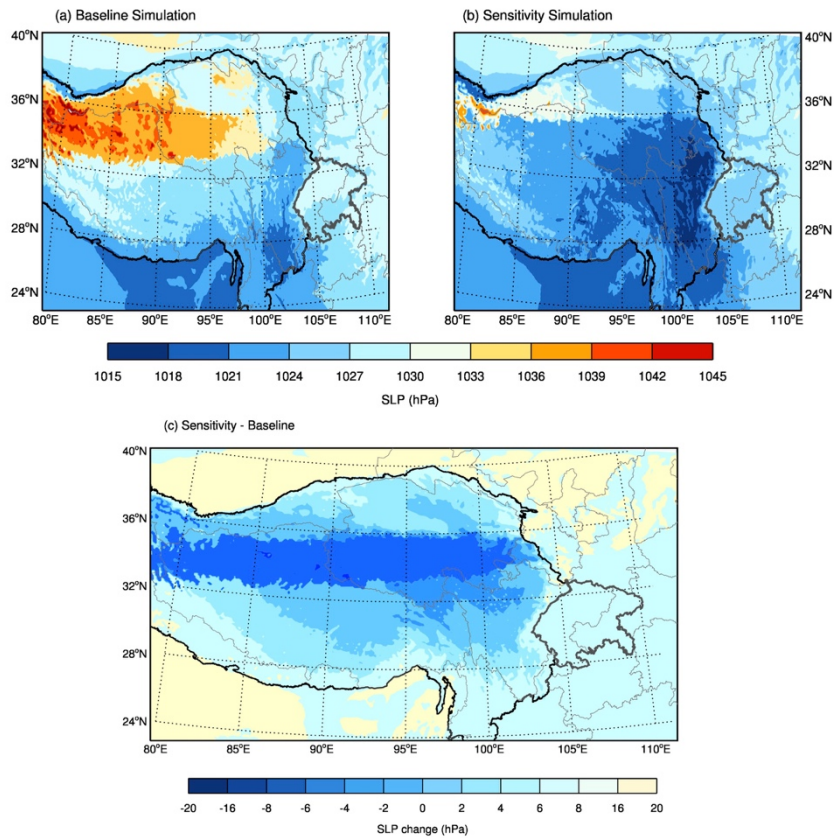
746

747

748

749

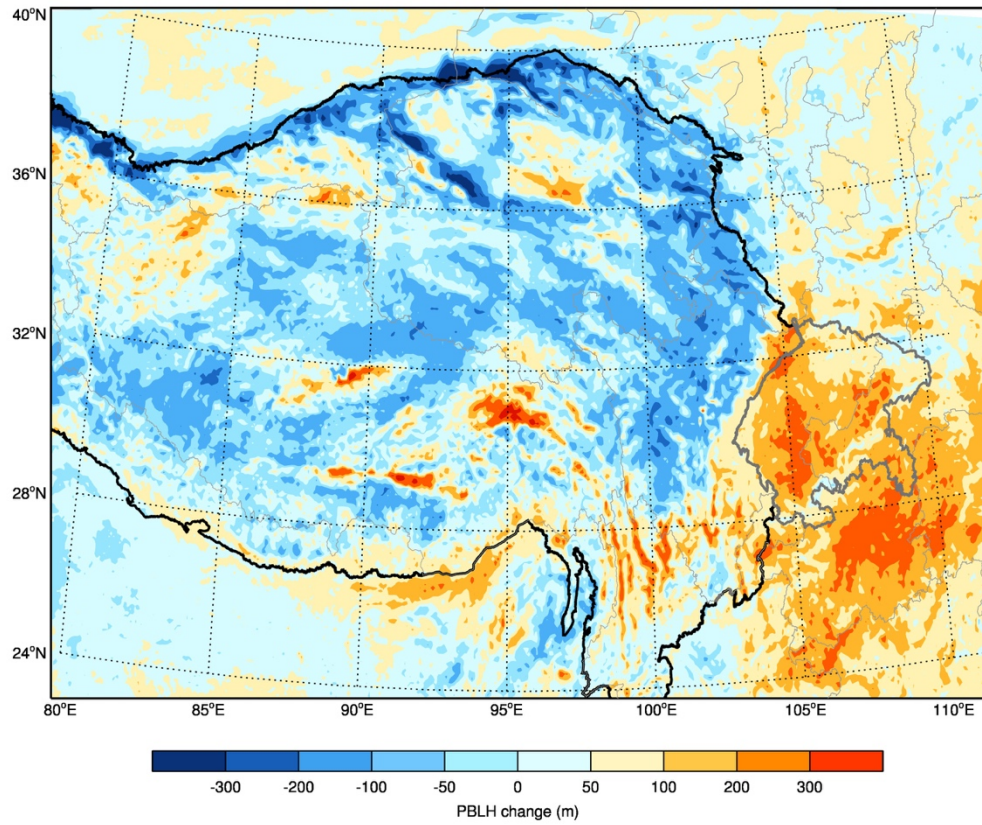
**Figure 7** Difference in spatial distributions of surface  $\text{PM}_{2.5}$  concentration (shading) and winds (arrows) between the sensitivity simulation and baseline simulation. The negative shows  $\text{PM}_{2.5}$  concentration decreases and the positive shows  $\text{PM}_{2.5}$  concentration increases when the Tibetan Plateau is  $2^\circ\text{C}$  warming.



751

752 **Figure 8** Comparison of spatial distributions of sea level pressure (SLP) between the (a)  
 753 baseline simulation and (b) sensitivity simulation over the Tibetan Plateau and Sichuan Basin.  
 754 (c) Changes in SLPs (sensitivity simulation *minus* baseline simulation) over the plateau and  
 755 basin while the plateau becomes 2°C warming.

756



758

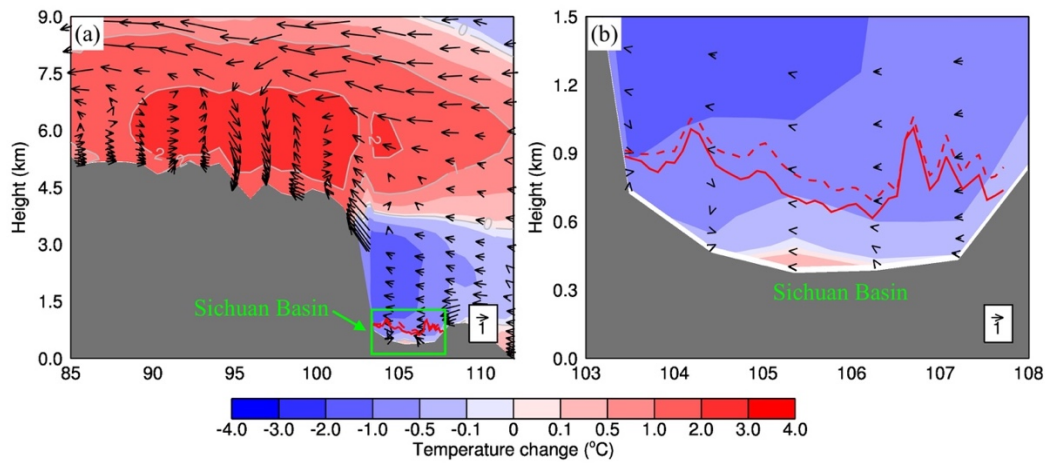
759 **Figure 9** Spatial change in the PBL height induced by 2°C warming over the **Tibetan Plateau**.

760 The positive shows the PBL height increases while the negative shows the PBL height

761 decreases.

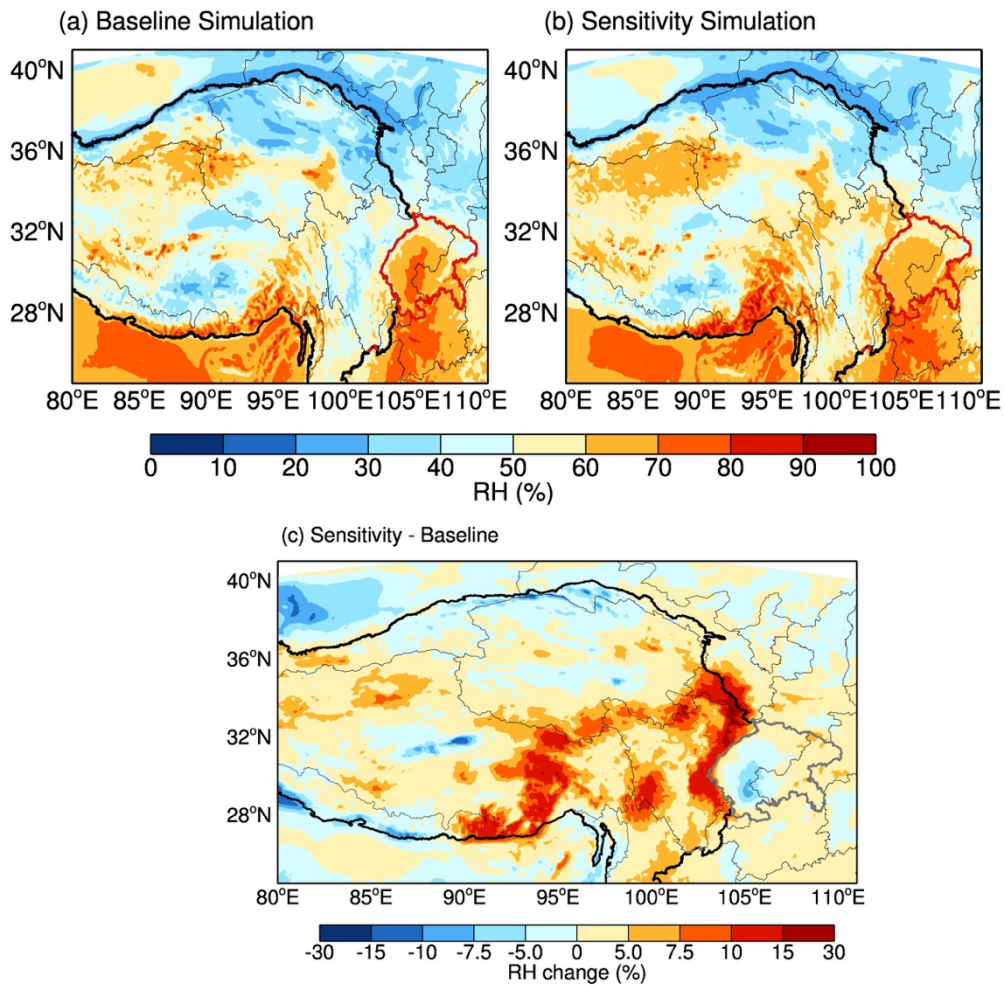
762

763



764

765 **Figure 10** Vertical profiles of changes in temperature (shading and gray contour) and  
766 winds (arrows) along 30°N in January 2014. The gray shaded area presents topography.  
767 The green box for the Sichuan Basin, and the red solid (baseline simulation) and dash  
768 (sensitivity simulation) lines for the PBL height. (a) The **Tibetan Plateau** and Sichuan  
769 Basin, and (b) The Sichuan Basin.



771

772 **Figure 11** Comparison of spatial distributions of RH between (a) baseline simulation  
 773 and (b) sensitivity simulation over the Tibetan Plateau and Sichuan Basin. (c) Similar  
 774 to Figure 9, but for RH spatial changes when the plateau becomes 2°C warming, and  
 775 the positive shows the RH increases while the negative shows the RH decreases.

776

777